International Journal of Biological Macromolecules, Volume 319, Part 4, August 2025, Article number 145691
DOI:10.1016/j.ijbiomac.2025.145691

Advanced Lignocellulose Bioprocessing for *Aloe vera* Leaf Rind through Novel Termite Gut Microbiome Consortia for Acetone Butanol Ethanol (ABE) Production: Metagenomics Insights and Process Economic Analysis

Gunasekaran Rajeswari[1], Vinod Kumar[1,2], Samuel Jacob[1*]

[1]Department of Biotechnology, School of Bioengineering, College of Engineering and Technology, Faculty of Engineering and Technology, SRM Institute of Science and Technology, SRM Nagar, Chengalpattu District, Kattankulathur-603203, Tamil Nadu, India

[2]School of Water, Energy and Environment, Cranfield University, Cranfield, MK43 0AL, UK

[*]Corresponding authors Email

samueljb@srmist.edu.in

Abstract

Consolidated bioprocessing (CBP) of lignocellulosic biomass (LCB) using microbes simplifies the process, eliminates enzyme cost and reduces the overall processing expenses. In this regard, termite gut, a potent reservoir of microbial symbionts produces various lignocellulolytic enzymes which acts synergistically to degrade LCB. However, the effectiveness of adapting the microbes with LCB for improved lignocellulolytic enzyme secretion and substrate degradation has been overlooked. Hence, in this study adaptive laboratory (ALE) of termite gut isolates was performed with various substrates such as saw dust (SD) and *Aloe vera* leaf rind (AVLR) under different conditions. Among the consortia, enriched termite consortium (ETC-3) showed the highest degradation of lignin (51.86 ± 2.03%, w/w), hemicellulose (29.27 ± 1.29%, w/w) and cellulose (41.97 ± 2.99%, w/w) with maximum specific enzyme activities. High throughput sequencing revealed the significant enrichment of Proteobacteria (88.95%) and Ascomycota (99.94%) groups in ETC-3. Further, the efficiency of ETC-3 in consolidated pretreatment and bioprocessing (CPBP) and CBP of AVLR towards acetone, butanol and ethanol (ABE) production was studied. Compared to the CPBP, CBP resulted in 1.6-fold higher glucose yield which subsequently enhanced the butanol yield (7.97 ± 0.40 g/L). Finally, cost benefit analysis ensured the economic feasibility of process strategies for AVLR valorization.

Keywords: *Aloe vera* leaf rind; Lignocellulose degradation; Microbial consortium

Published by Elsevier. This is the Author Accepted Manuscript issued with: Creative Commons Attribution License (CC:BY 4.0).
The final published version (version of record) is available online at DOI:10.1016/j.ijbiomac.2025.145691. Please refer to any applicable publisher terms of use.

1. Introduction

Bio-valorization of lignocellulosic biomass (LCB) by the synergistic action of complex lignocellulolytic enzymes (ligninase, hemicellulase and cellulase) is a promising alternative to the conventional pretreatment and saccharification (harsh chemicals and physical treatments) process. To date, several studies have focused on utilizing various lignocellulolytic enzymes for the degradation of lignin and polysaccharides in LCB owing to the high substrate specificity, absence of fermentative inhibitors and mild operating conditions [1-3]. However, multistep processing and high cost associated with the enzyme purification limits the techno-economic feasibility of LCB bio-valorization [4,5]. To circumvent these bottlenecks, consolidated bioprocessing (CBP), an ideal conversion strategy integrating the enzyme production, substrate hydrolysis and fermentation of sugars in a single stage (one reactor model) by microbes is progressively recognized as a suitable approach for bio-based products. The use of microbial systems in CBP for in-situ enzyme production can substitute the need for expensive enzymes, reduces the complexity, capital and operational cost of the process. Though recent studies have shown the feasibility of CBP, still it remained as a proof of concept owing to its major bottleneck such as development of an industrially viable microbial candidate (either single organism through strain engineering or consortium) that are effectively involved in the enzyme production, hydrolysis and fermentation in a single reactor. Other challenges include slow reaction rate, low product yield, incompatibility of optimal reaction conditions, limited control of the process and the need for an additional lignin removal step in LCB based biorefinery [https://www.celignis.com/bioprocess-cbp.php, 6, 7]. Therefore, CBP necessitates employing a robust microbial consortium which could mimic the degradation of plant biomass by synergistic action of microbial symbionts harboring sub-surface soils, compost, ruminants and termite guts [8-10].

Among the natural habitats, termite gut harbor ubiquitous syntrophic microbial communities that have evolved millennial years to tackle the recalcitrance of plant biomass. Termites, a eusocial insect can effectively digest upto 87% of hemicellulose and 99% of cellulose from a highly lignified hardwood [11,12]. In a termite colony, workers are the most abundant caste which are predominantly involved in foraging the wood as compared to the other castes such as reproductives (King and Queen) and soldiers. In addition, diverse microbial symbionts in the termite gut are possessed with a vast repertoire of ligninolytic and Carbohydrate active enzyme (CAZyme) [9, 13-15]. Hence, most of the studies are focused on culture dependent approach for the isolation of microbes from worker caste termite guts that are characterized with hemicellulolytic (xylanase) and cellulolytic (endoglucanase) activities [15-17]. This indicates that a group of microbial symbionts are synergistically involved in the degradation of lignocellulose. Lazuka et al. [18] employed 16S rRNA analysis of termite gut derived microbial consortium in order to reveal the wide spectrum of bacteria involved in carboxylates production from wheat straw. Compartmentalization of vital metabolic function through division of labor between symbionts and the prevalence of complex CAZymes profile could pave a way for bioprospecting to valorize LCB. Further, adaptive laboratory evolution (ALE) could be opted to enrich the microbial consortium with LCB to attain the intended functional characteristics [19,20]. ALE is widely used to evolve the microbes for enhancing the substrate utilization, enzyme secretion and tolerance to fermentative inhibitors [21,22].

Aloe vera leaf rind (AVLR), an agro-industrial waste constitutes a significant amount of lignin (19.12%, w/w), hemicellulose (15.57%, w/w) and cellulose (38.39%, w/w) which has been explored as a second generation feedstock for the production of ethanol [23,24], lactic acid and butanol [25]. Though proven to be effective in lab scale, employing conventional multi-step strategy (pretreatment, saccharification and fermentation) could be cost intensive. Production

of multiple products like acetone, butanol and ethanol (ABE) from AVLR by consolidating the process steps could fetch an economic feasibility in industrial scale.

Therefore, this study is focused on establishing an advanced lignocellulose bioprocessing for AVLR through microbial consortium for consolidated pretreatment and bio-saccharification (CPBS) by integrating lignocellulolytic enzymes production, pretreatment and hydrolysis in a single stage to improve the economic feasibility. To the best of authors' knowledge, this is the first study to inculcate ALE of termite gut derived microbial community using lignocellulosic substrates for improving the lignocellulolytic enzymes secretion and degradation. Followed by characterizing the vital symbionts and the microbial dynamics in native termite gut and enriched microbial consortium through high-throughput sequencing. The efficacy of potent microbial consortium in processing AVLR biomass was elucidated for ABE production by opting different process strategies:

Strategy I (Consolidated pretreatment and bioprocessing (CPBP)): Untreated AVLR biomass + Termite gut consortium + Fermentative strain (*Clostridium acetobutylicum* MTCC 11274)

Strategy II (CBP): Deep eutectic solvent (DES) pretreated AVLR biomass + Termite gut consortium + Fermentative strain (*C. acetobutylicum* MTCC 11274).

Finally, the cost-benefit analysis was performed to ensure the commercial feasibility of the opted strategies for the establishment of AVLR based biorefinery framework.

2. Materials and Methods

2.1. Lignocellulosic substrate

Saw dust (SD), a LCB generated during the wood processing was collected from the local sawmill situated in Chennai, Tamil Nadu, India. *Aloe vera* leaf rind (AVLR), a processing waste from aloe gel extraction was procured from the local unit located in Chennai, Tamil

Nadu, India. Then the fresh AVLR was solar dried, powdered, followed by sieving through a mesh to obtain 2 mm particle size and stored for further studies.

2.2. Termite collection and gut dissection

Termites from a single colony were collected from an old decaying wooden arboreal nest found in the province of Meenambakkam, Chennai, Tamil Nadu. A mixture of active termite caste along with the wooden pieces were randomly retrieved in dark and immediately transported to the laboratory. As the worker caste of termites are predominantly responsible for foraging, only the matured workers were chosen for the study and segregated from the soldiers and reproductives (King and Queen) based on the morphology (Fig. 1a). Then the workers were cold-immobilized, surface sterilized with 70% (v/v) ethanol, decapitated and the whole gut were dissected using a sterile fine tipped forceps under stereomicroscope [26]. The whole gut comprises foregut, midgut and hindgut (Fig. 1b and c). Each individual gut (n~100) were immediately pooled into an 8 mL cold phosphate buffer containing L-cystine hydrochloride (1%, w/v). The whole guts were then gently vortexed and the homogenates was used for further studies. In addition, to elucidate the native microbial symbionts of worker termites, the whole gut isolates (n~ 25) were immediately subjected to the DNA isolation as detailed in the section 2.5. A flow chart illustrating the standard operating procedure for termite collection and gut dissection is provided as supplementary Figure (Fig. S1). The termite was identified as *Odontotermes* sp. (belonging to Macrotermitinae subfamily) based on the morphology of the solider caste of termite. The head capsule is yellowish brown in colour, elongated and oval shaped (wider in the middle and converges anteriorly). Mandibles are slender, longer and black, whereas antennae found on the sides are brownish (Fig. 1a) [27,28].

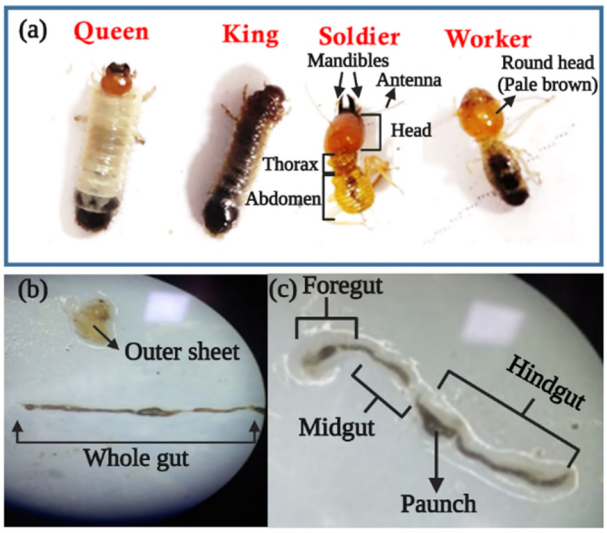


Fig. 1. Morphology of different castes of termites (a), isolation of termite gut (b) and the various segments of the isolated gut (c) sample

2.2.1. Termite gut inoculum (TGI)

The whole gut homogenate (8 mL) of workers was added in a serum vial containing minimal salt medium (MSM) (KCl - 0.5 g/L, $NaNO_3$ - 2.0 g/L, KH_2PO_4 - 1.0 g/L and $MgCl_2$ - 0.5 g/L) with 1% (w/w) of glucose as sole carbon source. The media is supplemented with trace elements (TE) (1 mL) and syringe filtered vitamin solution (1mL). The TE solution comprises the following constituents (g/L): $MnCl_2$- 0.05; H_3BO_3- 0.3; $CuCl_2$- 0.002; $ZnCl_2$- 0.042; $FeSO_4.7H_2O$- 0.1; $NiCl_2$- 0.024; $CoCl_2.6H_2O$- 0.19 and Na_2MnO_4- 0.018. The microbial culture was maintained at pH 7 with varied temperature i.e., mesophilic (37 ± 2 ˚C) and thermophilic (45 ± 2 ˚C) for 72 h under anaerobic condition. The anaerobic chamber was purged with inter gas (nitrogen) to remove the oxygen and the serum vials are sealed with rubber caps and aluminium crimp. The microbial culture is labelled as termite gut inoculum-mesophile (TGI-M) and termite gut inoculum- thermophile (TGI-T) and used for further adaptive laboratory evolution (ALE) studies.

2.3. ALE strategy for enrichment of microbes

ALE aids in the adaptation of isolated microbial consortia to the chosen LCB substrates such as SD and AVLR that constitutes a high and moderate amount of lignin and polysaccharides respectively. To obtain a stable microbial consortium with high lignocellulose degradation efficiency, sequential enrichment was performed in serum vials containing SD and AVLR as a sole carbon source at five different concentrations (0.5% (w/v), 1% (w/v), 1.5% (w/v); 2% (w/v) and 2.5% (w/v)) over 5 cycles with a regular incubation for 96 h. The gradual increment in the substrate concentration during ALE is to exert a selection pressure of heterogenous nature of LCB on the microbial communities during serial batch cultivations. This facilitates the gradual adaptation of microbes through metabolic rewiring to the complex substrate thereby enabling the evolution of microbial consortium with efficient substrate degradation capabilities. The enrichment medium constitutes MSM, TE and vitamin solution as mentioned in section 2.2.1. The adaptation of microbial symbionts was performed with 10% (v/v) of seed inoculum (TGI-M and TGI-T) under aseptic conditions. Additionally, a pure cellulosic substrate, such as commercial filter paper (FP) is used for the sequential enrichment of microbes to study the cellulolytic potential of different TGI in consolidated bio-saccharification (integrated cocktail hydrolytic enzymes production and saccharification using microbes). After 5 cycles of enrichment, the enriched microbial consortia were labelled as enriched termite consortium (ETC-1 to ETC-6) and the comprehensive experimental design for sequential enrichment are represented in the Fig. 2.

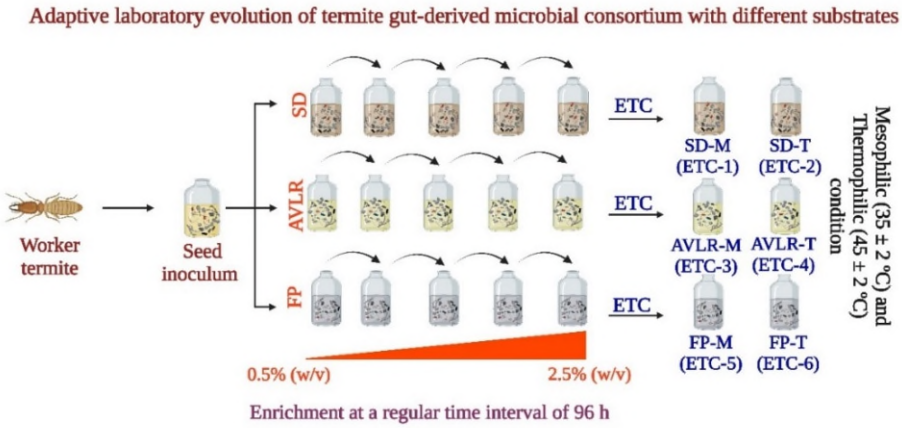


Fig. 2. A schematic representation of ALE strategy for enriching the microbial consortia derived from termite gut

2.4. Screening of enriched microbial consortia

Screening of potent microbial consortia was done based on the degradation potential using the chosen substrates (SD, AVLR and FP) with 10% (v/v) of ETC (1-6) as inoculum. All the experiments were performed in serum vials containing MSM, TE and vitamin solution as mentioned in section 2.2.1, followed by incubation for 7 days under different conditions (Table S1). The microbial culture obtained after the 5th enrichment cycle of ALE was used for the screening studies with the same substrate and enrichment conditions. After 7 days of microbial treatment, the samples were centrifuged at 8000 rpm, 4 °C for 10 mins. Then the solid residue and supernatant were used for the estimation of substrate degradation percentage, specific enzymes activities and sugar monomers respectively.

2.5. Genomic DNA extraction

The genomic DNA (gDNA) from the termite gut and the ETC-3 were extracted using the Nucleospin tissue (Macherey-Nagel, Germany) gDNA extraction kit according to the manufacturer protocol. The purity (A260/280) and the concentration of the gDNA was checked using Nanodrop spectrophotometer (Thermo Scientific, USA). An agarose gel (0.8%, w/v) electrophoresis was used to evaluate the gDNA integrity (Fig. S1 and Fig. S2).

2.6. Polymerase chain reaction (PCR) of 16S rRNA and Internal transcribed spacer (ITS) region

A specific primer targeting 16S rRNA (V3-V4 hypervariable region) and ITS regions were used for the PCR amplification of the eluted gDNA. The sequence of forward (F) and reverse (R) primers are as follows: variable region (V) V34F:- 5' AGAGTTTGATGMTGGCTCAG 3', V34R:- 5' TTACCGCGGCMGCSGGCAC 3' and ITSF:- 5' TTGGTCATTTAGAGGAAGTAA 3', ITSR:- 5' GCTGCGTTCTTCATCGATGC 3'. The reaction mixture (20 µL) consists of High-Fidelity DNA Polymerase enzyme with PCR reaction buffer, 10 pM primers and 40 ng gDNA. The PCR cycle conditions were set as follows: 94 °C for 2 min (initial denaturation), followed by 25 cycles at 95 °C for 15 s (denaturation), 56 °C for 15 s (annealing), and 72 °C for 2 min (elongation) with a final extension for 10 min at 72 °C. The resultant PCR product was purified using Gel/PCR purification kit (Qiagen, USA) and electrophoresed on an agarose gel (2.0%, w/v). Simultaneously the purity of amplicons was estimated using a Nanodrop spectrophotometer (Thermo Scientific, USA) [29].

2.7. Metagenomic library preparation and sequencing

The purification of the PCR amplicons was performed with AMPure XP (Beckman Coulter Inc., USA) to remove unused primers. In addition, index PCR (8 cycles) using Nextera XT Index Kit (Illumina, USA) was done to amplify the purified PCR products with Illumina barcoded adapters and dual indices. The metagenomic libraries were further purified using AMPure XP kit, and the concentration was estimated using Qubit dsDNA High Sensitivity assay kit (Thermo scientific, USA). The purified metagenomic libraries were normalized, pooled (4 nM concentration) and subjected to paired-end sequencing in Illumina Miseq using 2x300PE v3-v4/ITS sequencing kit [29].

2.8. Analysis of sequence data

The sequence analysis for 16S rRNA and ITS region was performed using Quantitative Insights Into Microbial Ecology (QIIME2-2021.4) software. After Illumina sequencing, the bcl data obtained was de-multiplexed and denoised followed by quality filtering. The 'Vsearch' plugin was used for joining the quality filtered reads, de-replicate sequence and clustering the features against the reference database (Greengenes (bacteria) and UNITE (fungi)). The identify threshold for the sequence was set at 97% and the taxonomy was assigned to the query sequences [30,31].

2.9. Process strategies for AVLR biomass valorization

To elucidate the efficiency of enriched microbial consortium (ETC-3) in processing AVLR biomass, two different strategies (strategy I: Consolidated pretreatment and bioprocessing (CPBP) and strategy II: Consolidated bioprocessing (CBP)) has been opted. CPBP integrates the various lignocellulolytic enzyme production, pretreatment, hydrolysis and ABE fermentation in a single reactor. Whereas in CBP strategy, AVLR is initially subjected to the DES pretreatment to partially removal the lignin and then the DES-pretreated AVLR is used as a carbon source in CBP strategy. For the DES pretreatment, most widely used Type-III DES composed of Choline chloride and Glycerol was synthesized and used for the pretreatment [32]. The DES pretreatment has selectively removed around 56% (w/w) of AVLR lignin, as reported in a previous study by author [25], leaving behind a solid residue rich in hemicellulose (14.50%, w/w) and cellulose (43.13%, w/w). Thus, enhancing the polysaccharide accessibility for microbial hydrolysis and increase the fermentable sugar yield.

In both CPBP and CBP, about 5 g of untreated or DES pretreated AVLR biomass was inoculated with 10% (v/v) of consortia (ETC-3) in a serum vial containing MSM, TE and vitamin solution as mentioned in section 2.2.1. The experiment sets were maintained under anaerobic condition at 37 °C for 96 h - 72 h based on the optimal sugar yield obtained from the

preliminary experiments. Followed by the inoculation of serum vial with 10% (v/v) of *C. acetobutylicum* MTCC 11274 for ABE production and the experiment sets were maintained at 37 °C for another 72 h under anaerobic condition. The chamber was purged with nitrogen gas and the serum vials are tightly sealed using rubber stopper and aluminium crimp. The intermittent sample was collected for every 24 h, followed by centrifugation (5000 rpm, 4 °C, and 20 mins) to separate the supernatant, which was used for the estimation of sugar monomers and ABE. The solid residue was oven-dried at 60 °C and stored in a zip lock cover for further characterization studies.

2.10. Analysis of substrate degradation

The structural cell wall components such as lignin, hemicellulose and cellulose for untreated and treated substrates were estimated using the standard protocol of National Renewable Energy Laboratory (NREL) and Anthrone method respectively [33-35].

2.11. Estimation of lignocellulose degrading enzymes

The activity of various enzymes such as laccase, manganese peroxidase (MnP), lignin peroxidase (LiP), xylanase, endoglucanase and total cellulase involved in lignin, hemicellulose and cellulose degradation are determined from the supernatant recovered after microbial treatment. For ligninolytic enzymes, various substrates such as veratryl alcohol, phenol red and 2,2′ - azino-bis(3-ethyl-benzothiazoline- 6-sulfonic acid) (ABTS) were used for estimating the LiP, MnP and laccase activity respectively [36-38]. Whereas total cellulase, xylanase and endoglucanase activity were measured using the respective substrates such as FP, xylan and carboxymethyl cellulose (CMC) [39,40]. The total protein content was determined by Bradford method and the specific enzyme activity is expressed as IU/mg (units of enzyme required to catalyse 1 µmole of substrates into product per min per mg of total protein) [41].

The enzyme activity is calculated based on the formula (Eq. 1 and Eq. 2) given below,

$$Ligninolytic\ activity\ \left(\frac{IU}{mL}\right) = \frac{\mathrm{A}\times V_{total}}{\varepsilon \times T \times V_{sample} \times l} \quad (1)$$

Where,

A = Absorbance of the product formed during the reaction at a specific wavelength (436 nm for laccase, 610 nm for MnP and 310 nm for LiP).

V_{total} = Total volume of the assay (mL)

Molar extinction coefficient (ε) = 22000 $M^{-1}cm^{-1}$ (MnP), ε =36000 $M^{-1}cm^{-1}$ (Laccase) and ε = 9300 $M^{-1}cm^{-1}$ (LiP)

T = Time (min)

V_{sample} = Volume of the sample (mL)

Pathlength (l) = 1 cm

$$Hemicellulolytic\ and\ cellulolytic\ activity\ \left(\frac{IU}{mL}\right) = \frac{Reducing\ sugar\ \left(\frac{mg}{mL}\right) \times Assay\ volume\ (mL)}{Molecular\ weight\ of\ \frac{xylose}{glucose}\left(\frac{g}{mole}\right) \times Time\ (\text{min}) \times Volume\ of\ enzyme\ (mL)} \quad (2)$$

The glucose or xylose concentration was calculated using the standard slope of pure glucose or xylose using dinitro salicylic acid (DNS) method [42].

The specific activity of enzymes was calculated using the Eq. (3) given below,

$$Specific\ enzyme\ activity\ \left(\frac{IU}{mg}\right) = \frac{Total\ enzyme\ activity\ \left(\frac{IU}{mL}\right)}{Total\ protein\ in\ the\ hydrolysate\ \left(\frac{mg}{mL}\right)} \quad (3)$$

Further, the presence of various extracellular enzymes in the supernatant were qualitatively determined using reverse phase-high performance liquid chromatography (RP-HPLC) (LC10ADVP, Shimadzu, Japan). All the samples were run under the condition as reported by Rajeswari et al. [43].

2.12. Estimation of fermentable sugar monomers

The liquid hydrolysate collected during the microbial treatment was subjected to the centrifugation (8000 rpm, 4 °C, 20 mins) to separate it from the solid biomass. Then the fermentable sugars (xylose, arabinose and glucose) in the liquid hydrolysate were determined using orcinol and DNS method respectively [42,44].

2.13. Estimation of ABE

Gas chromatography coupled with flame ionization detector (Agilent Technologies, USA) was used for determining the concentration of metabolites (ABE). Nitrogen was used as a carrier gas in the analysis. About 1 µL of sample was injected into the glass column operated at 220 °C, while the detector temperature was maintained at 300 °C. The concentration of the metabolites was calculated using the slope obtained from the standard graph (Fig. S3-S7) of acetone, butanol and ethanol (99.9% pure, Sigma-Aldrich, USA). Additionally, the productivity, yield coefficient and fermentation efficiency for acetone, butanol and ethanol were calculated using the formula as given in Eq. 4-6.

$$Product\ Productivtiy\ \left(\frac{g}{L.h}\right) = \frac{Maximum\ concentration\ of\ the\ product\ \left(\frac{g}{L}\right)}{Fermentation\ time\ (h)} \quad (4)$$

$$Product\ yield\ coeffecient\ \left(Y_{P/S}\right) = \frac{\Delta P}{\Delta S} = \frac{P - P_0}{S - S_0}\ (g/g) \quad (5)$$

ΔP = Change in concentration of the product (g/L)

ΔS = Change in concentration of the substrate (g/L)

$$Fermentation\ efficicency\ (\%) = \frac{Observed\ yield\ of\ the\ product\ \left(^{g}/_{g}\right)}{Theoretical\ yield\ of\ the\ product\ \left(^{g}/_{g}\right)} \times 100 \quad (6)$$

Theoretical yield of acetone - 0.32 (g/g of glucose), butanol - 0.41 (g /g of glucose) and ethanol- 0.51 (g /g of glucose)

2.14. Structural and morphological characterization of AVLR biomass

2.14.1. Fourier transform infrared (FTIR) analysis

To determine the variation in the functional group of untreated and treated AVLR biomass, FTIR analysis was performed (Agilent Technologies, Cary 600 Series, USA). The samples mounted by KBr pelleting method were scanned from 400-4000 cm^{-1} with 0.5 cm^{-1} spectral resolution [45].

2.14.2. X-ray diffraction (XRD) analysis

Crystalline nature of the AVLR biomass before and after treatment were analyzed using high resolution bench top XRD system (Malvern Panalytical, AERIS, UK) using CuKα radiation (α = 1.54 Å). The samples were scanned (2θ = 10 to 90°) with 3°/min speed and the diffraction profile was detected at 40 kV. Crystallinity index (CrI) percentage was calculated using the empirical formula (Eq. 7) for native cellulose as reported by Segal et al. [46]

$$CrI\ (\%) = \frac{I_{002} - I_{am}}{I_{002}} \times 100 \quad (7)$$

Where, I_{002} and I_{am} are the maximum (2θ- 22 and 23°) and minimum (2θ- 18 and 19°) intensity peak of crystalline cellulose respectively.

2.14.3. Scanning electron microscopy (SEM) analysis

The modification in the AVLR surface morphology during treatment was studied by SEM analysis (Model-FEI Quanta 200, USA). The dried samples were mounted on the stub and observed at 5 kV using SEM [47].

2.15. Cost-benefit analysis

The cost-benefit analysis was performed in accordance with Ozturk et al. [48] to determine the economic and industrial feasibility of various strategies (CPBP and CBP) opted for butanol production and lignin fractionation from AVLR. The plant capacity was assumed to process 1 Metric ton per hour (MTPH) of AVLR biomass and operates for 24 h a day over a span of 346 days in a year.

The direct fixed cost (DFC) of the plant are primarily comprised of total plant direct cost (TPDC), total plant indirect cost (TPIC) and contractor's fee and contingency (CFC) were calculated based on the Eq. 8-11.

$$DFC = TPDC + TPIC + CFC \quad (8)$$

$$TPDC = C_{IT} + C_{PP} + C_{PC} + C_{IN} + C_{EL} + C_{IL} + C_B + C_{AF} + C_{YI} \quad (9)$$

$$TPIC = C_{CO} + C_{EN} \quad (10)$$

$$CFC = C_{CF} + C_C \quad (11)$$

Where, C_{IT} - capital cost for instrumentation, C_{PP} - capital cost for process piping, C_{PC} - capital cost for equipment purchase, C_{IN} - capital cost for installation, C_{EL} - capital cost for electrical, C_{IL} - capital cost for insulation, C_B - capital cost for buildings, C_{AF} – capital cost of auxiliary facilities, C_{YI} - capital cost for yard improvement, C_{CO} - capital cost for construction, C_{EN} - capital cost for engineering, C_{CF} - capital cost for contractor's fee, C_C - capital cost for contingency.

On the other hand, the cost of raw materials, maintenance, utilities, labor, laboratory and other miscellaneous are included in calculating the annual operational expenses of the plant. The significant commercial economic notions such as net present value (NPV), payback period and internal rate of return (IRR) (Eq. 12-14) were used to determine the probability of products.

$$\text{NPV} = -\text{DFC} + \sum_{t=1}^{20} \frac{Cash\ flow\ (CF)}{(1+i)^t} \quad (12)$$

$$0 = NPV = \sum_{t=1}^{20} \frac{CF}{(1+\text{IRR})^t} - DFC \quad (13)$$

$$Payback\ \text{period} = \frac{DFC}{CF} \quad (14)$$

Where,

i - discount rate,

t - project time

Further, sensitivity analysis of NPV was carried out to avoid any financial risk and to resolve the uncertainty in plant feasibility. For this analysis, varied market conditions such as discount rate (2-8%), project lifetime (15-25 years) and income tax (15-25%) were considered as a parameter.

2.16. Statistical analysis

All the experiments were done in triplicates and the results are represented as the average of the three independent trails. The standard deviation denoted as (±) was calculated from the mean of these trials.

3. Results and discussion

Recently, microbial consortium based valorization of LCB serves as a promising avenue for integrating the multiple steps including secretion of various ligninase and CAZymes involved in lignocellulose breakdown, pretreatment and hydrolysis of polysaccharides into fermentable sugar monomers [49]. In this regard, among the ecological niches, the ubiquitous microbial symbionts of termite guts are possessed with a vast repertoire of ligninolytic and CAZymes which are responsible for the complete degradation of lignocellulose [9]. For this reason, termites are considered as a desired model for industrial bioprospection of LCB. Further, performing ALE over a defined period under various conditions could aid in acclimatizing the microbes to effectively degrade LCB [50]. Nevertheless, studies have never explored the effectiveness of ALE for enriching the termite gut derived microbial communities using woody biomass (SD) and agro-industrial waste (AVLR) to develop a robust microbial consortium for consolidating the multi-step treatment strategies of LCB into a single process.

Therefore, this is the first study to focus on establishing a microbial consortium for CPBS using ALE strategy with the chosen model substrates (SD and AVLR). Followed by probing the vital key players in native termite gut microbiome and enriched microbial consortium (ETC-3) through high-throughput sequencing. In addition, the study also aims to establish different process strategies (CPBP and CBP) for AVLR valorization using ETC-3 for ABE production along with a cost-benefit analysis for the industrial and economic feasibility.

3.1. Taxonomic annotation of microbial community in native termite gut microbiome

To annotate the bacterial and fungal diversity in the termite gut, a pair-end amplicon (16S rRNA and ITS) sequencing was performed using Illumina MiSeq platform. A total of 34 and 18 million base pair was generated in 16S rRNA and ITS sequencing with a GC content of 53% and 51.5% respectively. The bacterial and fungal communities were taxonomically

annotated and the relative abundance was represented at the top 10 phylum, family, and genus levels (Fig. 3 a and b).

3.1.1. Bacterial population in the termite gut

Based on the 16S rRNA sequencing analysis (Fig. 3a), Bacteroidetes (38.24%) were the most dominant phylum colonizing the termite gut followed by Firmicutes, Synergistetes, Proteobacteria, Planctomycetes, Planctomycetes, Spirochaetes and Actinobacteria with a relative abundance of 22.19%, 11.31%, 9.82%, 8.25%, 6.79% and 2.24% respectively. Moreover, *Rikenellaceae* (36.98%), *Lachnospiraceae* (17.90%) and *Dethiosulfovibrionaceae* (12.27%) were the significant family taxon identified in the termite gut. At the genus level, only *TG5*, *Treponema*, *Dysgonomas* and HA73 were classified with a relative abundance of 10.10%, 7.84%, 2.66% and 2.80% respectively. However, a significant proportion of the bacterial genera in termite gut remained unclassified across various OTUs as shown in the Fig. 3(a), suggesting the microbiome complexity. These unclassified genera were associated with the bacteria from different phyla, classes, orders, or families found in the termite gut. Several studies have reported that Bacteroidetes in termite gut are involved in the polysaccharide breakdown by the prevalence of CAZyme encoding gene of Glycoside hydrolase (GH) family (xylanase and endoglucanase) [51-56]. While, Auxiliary activities (AA) enzyme genes associated with the lignin degradation are predominant in Proteobacteria phylum [57]. The members of the Actinobacteria phylum, predominant in the termite foregut and midgut are possessed with the diverse ability of metabolizing lignin and cellulose by secreting extracellular peroxidase and cellulase [29, 52, 58, 59]. Kohler et al. [60] investigated that many species from Firmicutes (*Lachnospiraceae* family) in *Nasutitermes corniger* showed high xylanolytic activity indicating its ability in hemicellulose degradation. Spirochetes are one among the phyla present in both the lower (*Tsaitermes ampliceps*, *Reticulitermes flaviceps* and *R. speratus*) and higher wood-feeding termites (*Microcerotermes parvus* and *N. corniger*)

which are associated with the high abundance of putative GH genes involved in the degradation of cellulose [12, 61-63]. The genus *Treponema* belonging to the phylum Spirochaetes are possessed with numerous Fe-hydrogenases that produce molecular H_2 as by-product during the anaerobic fermentation of carbohydrates [60, 64].

3.1.2. Fungal population in termite gut

In termite gut, Ascomycota was the most predominant phylum with 66% of the sequence reads followed by Basidiomycota with 34%. A distinct profile of fungal families has been identified in the termite gut (Fig. 3b), where *Vuilleminiaceae* (27.53%) belonging to the order Helotiales was the most abundant family. This is followed by *Trichomonascaceae* and *Mycosphaerellaceae* families each representing 16.10% of the total population. Meanwhile, a diverse range of significant genera such as *Vuilleminia* (27.89%), *Phialotubus* (18.01%), *Termitomyces* (13.02%) and *Aspergillus* (11.42%) were identified in the fungal community. Earlier studies have revealed that *Termitomyces* and *Vuilleminia* are possessed with the AA1 laccase, AA2 versatile peroxidase and AA9 lytic polysaccharide monooxygenase genes that are involved in metabolizing LCB [65-68]. Whereas, various species of *Aspergillus* genus are reported to produce a cocktail of xylanase (carbohydrate esterase (CE) and GH families) and cellulase (GH family) signifying the polysaccharides degradation capability [69,70].

Therefore, the metagenomic analysis of termite gut revealed that phyla Bacteroidetes, Firmicutes, Actinobacteria, Proteobacteria, Ascomycota and Basidiomycota are possessed with CAZymes (Families of GH and CE), cellulosome and AA enzymes namely AA2 versatile peroxidase and AA1 laccase which are involved in the degradation of polysaccharides and lignin respectively [67, 70-73]. Further, ALE of termite gut derived microbes with LCB could enable the development of microbial consortium suitable for CPBS.

3.2. Selective enrichment of microbial community through ALE with diverse lignocellulosic substrates

The adaptation of the termite isolates (TGI-M and TGI-T) was performed with different substrates namely SD, AVLR and FP as a sole carbon source. The substrate concentration was varied incremental from 0.5 to 2.5% (w/v) in the 5 sequential cycles of ALE. At the end of sequential cycles, the screening of potent LCB degraders was done based on the specific enzyme activity and the subsequent degradation potential of the enriched consortium (ETC- 1 to 6) in the respective substrates and the conditions opted (mesophilic/thermophilic) for enrichment strategy.

3.2.1. Screening of termite gut-derived enriched microbial consortium

For the screening of potent consortia, the degradation percentage of structural components of substrate (lignin, hemicellulose and cellulose) and the specific enzyme activity of various extracellular lignocellulolytic enzymes (laccase, LiP, MnP, xylanase, endoglucanase and total cellulase) were determined for different ETC (1 to 6) under different treatment conditions as shown in Table S1. From the Fig. 4(a), it has been observed that among the treatment sets utilizing lignocellulose, ETC-3 treatment showed higher degradation of lignin (51.86 ± 2.03%, w/w), hemicellulose (29.27 ± 1.29%, w/w) and cellulose (41.97 ± 2.99%, w/w) of AVLR biomass with higher specific enzyme activities (laccase- 33.23 ± 1.39 IU/mg, Mnp-7.52 ± 0.76 IU/mg, LiP- 7.95 ± 0.62 IU/mg, total cellulase- 1.94 ± 0.26 IU/mg, endoglucanase- 15.30 ± 0.77 IU/mg and xylanase- 1.52 ± 0.26 IU/mg (Table 1). However, ETC-5 and ETC-6 showed a higher cellulose degradation of about 57.06 ± 3.28% (w/w) and 43.54 ± 2.58% (w/w) respectively owing to the substrate (FP) with pure cellulose content. Additionally, the secretion of MnP, LiP, xylanase and cellulase by various enriched consortium (ETC) were analyzed by HPLC. The retention time of pure enzyme standards were determined in a previous study by author [43] and correlated with the retention time obtained from the chromatogram profile of

various enzymes secreted by the enriched microbial consortium (Fig. S8). A summary table correlating the retention time of enzyme standards and samples are provided in the Table S2.

On the other hand, different ETC treatment have resulted in the yield of various sugar monomers such as arabinose, xylose and glucose (Fig. 4b-d). A maximum sugar yield of about 104.49 ± 4.72 mg/g (xylose), 28.40 ± 2.65 mg/g (arabinose) and 150.83 ± 6.21 mg/g (glucose) was obtained upon ETC-3 treatment of AVLR biomass. Whereas, FP treatment with ETC-5 has resulted in a maximum of 167.38 ± 5.59 mg/g of glucose. Thus, the yield of sugar monomers obtained after ETC treatment was correlated with the specific activity of various lignocellulolytic enzymes involved in the substrate degradation.

In a nut shell, ETC-3 was found to be a potent consortium with the highest degradation percentage of AVLR biomass resulting in the maximum sugar yield when compared to the different ETC's treatment sets with LCB. The efficiency of the ETC-3 in degradation of AVLR cell wall components was compared with the other reported studies [8, 74-77] as provided in the Table S3.

3.3. Elucidation of potent microbial consortium based on enzymatic degradation potential through Principle component analysis (PCA) and Spearman correlation analysis

3.3.1. PCA

In order to evaluate the correlations and similarities among enriched microbial consortia (ETC) in degrading various substrates, a multivariate PCA was performed (Fig. 4e). The multidimensional scaling of datasets in PCA assists in identifying the significant patterns of microbial consortia based treatments. The ordinations of variables such as specific enzyme activities and the structural components degradation percentage of substrates are considered for PCA.

Clustering of ETC accounted for 97.3% of observed variability with principle component (PC) 1 and PC2 contributing 73.2% and 24.1% respectively as shown in Fig. 4(e). In the PCA biplot,

1 out of 6 ETC samples (i.e., ETC-3) revealed a strong positive correlation for the estimated MnP, LiP and xylanase specific activities along with the degradation of AVLR lignin and hemicellulose. While, ETC-5 are highly active for endoglucanase and total cellulase specific activities which in turn resulted in the 57.06 ± 3.28% (w/w) of FP degradation. Hence the cellulose degradation was higher for FP substrate as compared to other ETC treatment with LCB. Notably, AVLR treatment with ETC-3 has resulted in 41.97 ± 2.99% (w/w) of cellulose degradation which was found to be higher than the other treatment sets with LCB.

Overall, a significant positive correlation ($cos2>0.95$) was observed for ETC-3 treatment based on the secretion of cocktail enzymes that effectively degraded the AVLR biomass. Similarly, the effectiveness of bacterial consortia in LCB degradation was assessed by Sadalage et al. [78] among the 10 synthetic consortia, CM10 was determined to be the most promising consortium in grass straw degradation based on the PCA biplot analysis.

3.3.2. Spearman correlation analysis for enriched microbial consortia

To identify the most potent consortium, Spearman correlation heat map was plotted to evaluate the relationship between the various enriched microbial consortia, substrate degradation and the sugars yield. In the correlation Figure 4 (f and g), various ETC represents the total of the respective specific lignocellulolytic enzyme activities determined after treatment. Similarly, the degradation percentage of structural components and the sugars yield were combined to represent the substrate degradation percentage and sugars yield respectively.

From the correlation analysis, the experimental set ETC-3 and ETC-5 carried out using AVLR and FP as a substrate showed a significant positive correlation with both the chosen variables (i.e., substrate degradation and sugars yield) as compared to the other counter parts (Fig. 4f and g). Among the positively correlated consortia, ETC-3 showed a higher level of significance with both substrate degradation ($r = 0.8$ and $p < 0.01$), and sugars yield ($r = 0.8$ and $p < 0.001$).

Together PCA and correlation analysis clearly revealed that ETC-3 from termite gut was the most promising consortium for the LCB degradation and was chosen for further studies.

3.4. Comparative analysis of native termite gut and AVLR-enriched microbial communities through high throughput sequencing

The diversity and the relative abundance of bacterial and fungal population in AVLR-enriched termite gut microbial consortium (ETC-3) were assessed by 16S rRNA and ITS region amplicon sequencing respectively. Then the comparative analysis of bacterial and fungal population in native termite gut microbiome and the ETC-3 were represented at the phylum and order level (Fig. 5a-d).

3.4.1. Bacterial and fungal taxonomic diversity profile

The relative abundance of the bacterial population in native termite gut and ETC-3 were taxonomically annotated at the phylum and the order level. From the Fig.5 (a and b), it was observed that upon sequential adaptation of microbial consortium with AVLR biomass, the bacterial population was remarkably altered in ETC-3 which is largely dominated by the Proteobacteria (88.95%) and Firmicutes (10.97%). Meanwhile, Enterobacteriales (88.64%), Bacillales (10.60%) and Lactobacillales (0.31%) are significantly enriched in ETC-3 among the other orders (Clostridiales, Rhizobiales, Sphingomonadales, Caulobacterales, Xanthomonadales, Pseudomonadales and Burkholderiales) found in native termite gut. Similarly, the fungal community has become radically distinct in ETC-3 with Ascomycota comprising 62,477 OTUs as the highly prevalent phylum (Fig. 5c and d). Saccharomycetales, Eurotiales, Agaricostilbales, Hypocreales and Trichosphaeriales are the common orders identified in both the native termite gut and ETC-3. Among these taxon members, Saccharomycetales (99.65%) which belongs to the class Saccharomycetes was vastly enriched in the ETC-3 sample.

3.5. Core microbes in enriched termite gut consortium

The taxonomic annotation of core microbes in ETC-3 were illustrated as an alluvial diagram (Fig. S9). In bacterial community, the most abundant phyla Firmicutes and Proteobacteria are majorly classified under Alphaproteobacteria, Betaproteobacteria, Gammaproteobacteria, Bacilli and Clostridia respectively. These classes of bacteria are known to possess a large repertoire of CAZymes, cellulosome system and extracellular peroxidase for metabolizing LCB [79-81]. Notably, the enriched families upon AVLR sequential adaptation includes *Enterobacteriaceae, Bacillaceae*, *Streptococcaceae*, *Clostridiaceae*, *Bacteroidaceae* and *Sphingomonadaceae*. The identified genera in ETC-3 namely *Bacillus* and *Bacteroides* are widely reported for its lignin degrading abilities [82-84]. Whereas, *Clostridium* species are well-known for its cellulosome system comprising a wide variety of saccharolytic enzymes (hemicellulase and cellulase) for consolidated bio-saccharification of LCB [81]. Among fungi, *Candida* genera is highly prevalent and has been reported as an opportunistic yeast in metabolizing the lignin and xylose [16,85]. Other taxon members including *Penicillium*, *Sterigmatomyces* and *Xeromyces* are found to aid in the LCB degradation through the production of ligninase, hemicellulase and glucosidases [86].

The enrichment of Proteobacteria and Ascomycota population in ETC-3 might be attributed to the potential synergism in AVLR degradation. For example, *Pseudomonadaceae* are known to secrete an array of diverse ligninolytic enzyme such as laccase, LiP and MnP that aids in the lignin degradation, thereby enhancing the accessibility of polysaccharides [Xu et al., 2022; Zhou et al., 2025; Grgas et al., 2023]. Then the lignin-derived aromatic compounds are efficiently metabolized by another group of bacteria such as *Burkholderiaceae* and *Caulobacteraceae* through the cleavage of aromatic rings, in turn facilitates the other bacteria or fungal growth and enzyme activities [Wilhelm et al., 2019; Morya et al., 2021]. Similarly, the members of the bacterial (*Enterobacteriaceae*) and fungal (*Aspergillaceae and*

Trichocomaceae) communities secretes a cocktail of hemicellulase and cellulase that act in concomitant during the polysaccharide breakdown [Luo et al., 2024; Sahu et al., 2025; Boondaeng et al., 2024; Devi et al., 2024; Chen et al., 2024]. Further, *Fusarium* belonging to *Nectriaceae* family enhances the saccharification of cellulose by secreting β-glucosidase that are involved in the hydrolyses of cellobiose into glucose [Bertonha et al., 2018]. The synergistic mechanism between the bacterial and fungal population might be owing to the (i) enzyme synergy (several microbes contributes to the diverse enzymes secretion for complete substrate degradation) and (ii) growth synergy (interactions of signalling molecules or secondary metabolites between microbial groups) [Taha et al., 2015, Ren et al., 2015; Detain et al., 2024]. Therefore, the enrichment of Proteobacteria and Ascomycota in ETC-3 are found to be associated with the cooperative enzyme production by diverse group of bacteria and fungi, ensuring concerted AVLR lignocellulose degradation.

3.6. Correlation between AVLR structural components degradation, fermentable sugars yield and enriched microbial consortium (ETC-3)

Pearson correlation and Mantel test coefficients were used for analyzing the relationship between the AVLR structural components degradation, fermentable sugar monomers yield and the relative abundance of the ETC-3 (order level) respectively (Fig. 6a and b). As a result of microbial consortium treatment, a positive correlation was observed between the breakdown of AVLR structural components and the release of sugar monomers. The AVLR lignin breakdown showed a positive correlation coefficient (r) of about 0.99 and 0.38 for pentose sugars (xylose and arabinose) and glucose respectively, indicating that the lignin removal improves the polysaccharide accessibility. Consequently, the breakdown of hemicellulose and cellulose to pentose sugars (0.98) and glucose (0.97) showed a very strong positive correlation. Then, for the Mantel ‘r’ test, a singular value for the relative abundance of the microbes was considered (a limitation of the study) and the test was performed to evaluate the correlation

between the relative abundance of the microbial consortium and AVLR degradation, along with the sugars yield. In the enriched bacterial community (Fig. 6a), the relative abundance of the Enterobacterales was positively correlated with degradation of AVLR structural components and sugars yield with 'r' values ranging from 0.25 to 0.5. Notably, Enterobacterales harbours a diverse CAZymes profile signifying the vital role of ETC-3 in efficient AVLR degradation [87]. Xanthomonadales and Actinobacteria are positively correlated with the AVLR lignin and hemicellulose degradation along with the pentose sugars yield, whereas glucose yield correlates with the Bacteroidales. Other bacterial lineages in ETC-3 either had no or minimal effect on the degradation of AVLR biomass and the sugar yield, where the 'r' values were less than 0.25.

Similarly, in the fungal population (Fig. 6b), Saccharomycetales exhibited a positive correlation which clearly emphasized that yeast perhaps aid in the AVLR degradation by the secretion of potential cocktail enzymes such as ligninase and cellulase [88,89]. While, other fungi including Eurotiales, Agaricostillbales, Hypocreales and Trichospaeriales had no or minimal effect on these variables. Therefore, the complexity of symbionts interaction within the ETC-3 is characterized by the distinct relationship between certain microbial populations and the AVLR biomass.

3.7. Different process strategies for AVLR biomass valorization

As ETC-3 are possessed with a diverse group of microbes with a concoction of various lignocellulolytic enzymes, the microbial consortium efficiency in valorizing AVLR biomass for ABE production was studied by opting different process strategies such as CPBP and CBP. CPBP integrates the enzyme production, pretreatment, saccharification and subsequent ABE fermentation in a single bioreactor which simplifies the overall process, enhances the conversion efficiency and reduces the processing time and costs [6]. Further to enhance the commercial feasibility of microbial consortium-based AVLR valorization and to provide a

balance between the process efficiency and cost economics, a subtle and green chemical like DES was chosen as a pretreatment agent. The DES synthesized using choline chloride and glycerol has selectively removed around 56% (w/w) of AVLR lignin as reported in a previous paper by author [25]. This selective fractionation of AVLR lignin would intensifies the polysaccharides availability for subsequent saccharification and fermentation mediated by microbial consortium in a single pot. Thus, the untreated and DES treated AVLR biomass were used a sole carbon source in CPBP and CBP strategies respectively.

Preliminary experiments were performed to determine the optimal time in attaining the maximum enzyme activity and sugar yield by analyzing the dynamic profile of various lignocellulolytic enzymes and the sugar monomers at a regular time intervals (every 24 h) in ETC-3 mediated valorization of untreated and DES- treated AVLR biomass. This would aid in the subsequent addition of fermentative strain (*C. acetobutylicum* MTCC 11274) into the CPBP and CBP set for ABE production. Based on the preliminary results (Fig. S10 and Fig. S11), maximum specific activity of various enzymes and the sugar yield was observed at the 96 h and 72 h of ETC-3 mediated CPBP and CBP strategies respectively. Therefore, CPBP and CBP was carried out for 168 h and 144 h respectively: first 96 h (CPBP) and 72 h (CBP) involve the pretreatment and hydrolysis of biomass using ETC-3 to achieve the maximum sugar yield followed by the addition of *C. acetobutylicum* MTCC 11274 to convert the sugar monomers into ABE in next 72 h.

3.7.1. Effect of microbial consortium mediated CPBP and CBP on AVLR degradation and sugars yield

The influence of ETC-3 on lignin, hemicellulose and cellulose degradation in untreated and DES treated AVLR biomass and the production of various sugar monomers (xylose, arabinose and glucose) was studied. From the Fig. 7(a), it was observed that a significant percentage of lignin (52.93 ± 1.08%, w/w), hemicellulose (29.60 ± 0.98%, w/w) and cellulose (43.00 ±

1.90%, w/w) was removed from AVLR biomass after ETC-3 mediated CPBP. This result highlights the synergistic action of various lignocellulolytic enzymes secreted by ETC-3 in the efficient breakdown of cell wall components of the AVLR biomass. Similar to this study, simultaneous pretreatment and hydrolysis of wheat straw using termite gut derived microbial consortium (*Bacillus* sp. BMP01 and *Ochrobactrum oryzae* BMP03) has resulted in 44.47% and 49.58% of delignification and saccharification respectively [90]. However, microbial consortium derived from *Nasutitermes lujae* species of termites has degraded 37.27% (w/w) of lignin and 55.48% (w/w) of cellulose in wheat straw [77].

Whereas, in CBP of DES pretreated AVLR a maximum delignification of about 60.94 ± 1.87% (w/w) was obtained with 33.20 mg/g of residual lignin. Among the process strategies (Fig. 7b), the degradation percentage of hemicellulose (48.62 ± 2.33%, w/w) and cellulose (82.14 ± 3.13%, w/w) was significantly higher in CBP of AVLR biomass. Thus, the DES pretreatment has selectively fractionated the AVLR lignin (86.20 ± 2.45 mg/g) thereby enhancing the polysaccharides availability for microbial hydrolysis which resulted in enhanced removal of hemicellulose and cellulose.

On the other hand, the hydrolytic potential of ETC-3 in producing fermentable sugar monomers from untreated and DES treated AVLR biomass revealed that glucose yield was higher as compared to xylose and arabinose at the optimal time of CPBP (96 h) and CBP (72 h) (Table 2). Moreover, a 1.27-fold increase in the saccharification percentage was obtained in the CBP of DES pretreated AVLR (63.75 ± 2.54%, w/w) compared to the CPBP of AVLR biomass (49.82 ± 1.77%, w/w). Similarly, separate pretreatment and hydrolysis of rice straw using termite gut-derived microbial consortium has resulted in enhanced saccharification of about 69.96% (w/w) with 440 mg/g of reducing sugar [91].

3.7.2. ABE production

During ETC-3 mediated CPBP and CBP, *C. acetobutylicum* MTCC 11274 was added to the serum vial at the optimal time of maximum sugar release (CPBP- 96 h and CBP-72 h) to utilize the AVLR derived sugar monomers for ABE production. From the Fig. 7(c and d), it was observed that a decrease in the concentration of sugars has resulted in the maximum yield of acetone, butanol and ethanol at 72 h of fermentation in both CPBP and CBP strategy. During ABE fermentation, butanol titer was found to be significantly increased and higher as compared to the other products in the mixture. In CPBP strategy, a maximum yield of about 5.45 ± 0.37 g/L of butanol was achieved with a productivity and yield coefficient of around 0.07 ± N.D g/L.h and 0.29 ± 0.02 g/g of glucose respectively (Fig. 7c and Table 3). However, in CBP set, the yield (7.97 ± 0.40 g/L), productivity (0.11 ± N.D g/L.h), yield coefficient (0.32 ± 0.02 g/g of glucose), and fermentation efficiency (77.56%) of butanol were observed to be higher as compared to the CPBP of AVLR biomass (Fig. 7d and Table 3). The results obtained in this study was found to be slightly higher than the other reported study where batch fermentation of de-oiled rice bran derived glucose has resulted in 7.53 g/L of butanol with 0.25 g/g and 0.105 g/L.h of yield coefficient and productivity respectively [92]. At the commercial scale, an optimal total ABE concentration of about 20 g/L was reported to be typically produced from 55 to 60 g/L of sugar upon traditional ABE fermentation using industrial Clostridium strains [Jones and Keis, 1995; Green, 2011]. A full-scale industrial ABE fermentation using *C. acetobutylicum* has resulted in an optimal butanol yield (12 g/L) with 20 g/L of total solvent yield using maize as a carbon source [Gabriel and Crawford, 1930; Jones, 2024]. Similarly, several *C. saccharobutylicum* strains has attained a butanol yield ranging from 12 to 13.2 g/L as reported by various companies such as National Chemical Products (South Africa), Commercial Solvents Corporation (US), Commercial Solvents Ltd. (UK) and Green Biologics Ltd. (US). However, various factors including the specific strain (*C. acetobutylicum, C.*

beijerinckii, C. saccharoperbutylacetonicum and *C. saccharobutylicum*), type of substrate (sugar (molasses) or starch (maize, cassava, corn and sweet potato)) and fermentation condition could significantly vary the product yield [McCutchan and Hickey, 1954; Walton and Martin, 1979; Ross, 1961; Ryden, 1958; Jones, 2024]. The maximum butanol yield (CPBP- 5.45 g/L and CBP- 7.97 g/L) obtained in this study was comparatively less than the optimal industrial yields. Nevertheless, the butanol yields were within the standard tolerance limit (~13 g/L) for *C. acetobutylicum* under batch fermentation [Ryden, 1958].

3.8. SEM, XRD and FTIR analysis of untreated and treated AVLR biomass

To study the extent of structural and functional group modification in AVLR biomass before and after various treatment strategies (CPBP and CBP), SEM XRD and FTIR analysis was performed (Fig. 8a-c).

From the SEM analysis (Fig. 8a), the cell wall surface of untreated AVLR biomass was observed to be smooth, highly intact and well structured, whereas CPBP and CBP of AVLR biomass has resulted in the surface irregularity and roughness indicating the disintegration of cell wall components.

Cellulose crystallinity, a key structural characteristic signifying the effect of microbial consortium in AVLR degradation was determined by calculating the CrI percentage from the XRD spectra. From the Fig. 8(b), a reduction in the CrI value to 23.89% and 18.29% was observed after CPBP and CBP of AVLR respectively, as compared to the untreated biomass (CrI - 25.44%). This might be due to the concerted action of lignocellulolytic enzymes involved in degrading the crystalline and amorphous region of AVLR biomass. Similarly, a decrease in the crystallinity index of Kans grass and *Miscanthus sinensis* after enzyme treatment was reported in previous studies [93,94].

The modification in the functional group of AVLR biomass in response to the various process strategies was determined by FTIR analysis (Fig. 8c). The spectra observed around 3300 cm^{-1},

2912-2902 cm^{-1} and 1149 cm^{-1} are attributing to the O-H, C-H, C-O-C and C-C bonds stretching vibration respectively [95]. The characteristic peaks of lignin, hemicellulose and cellulose were evident in the untreated AVLR biomass by the bands around the region 1411 cm^{-1}, 2920 cm^{-1} and 1111 cm^{-1} respectively. However, decrease in the intensity or elimination of the spectral bands (1400 cm^{-1}, 1298 cm^{-1} and 2902 cm^{-1}) upon CPBP and CBP of AVLR biomass are corresponding to the lignin monomeric units (syringyl and guaiacyl) stretching vibrations, C-C stretching and C-H deformation in cellulose unit [96,97].

3.9. Cost-benefit analysis of process strategies opted for AVLR valorization

To study the industrial and economic feasibility of various strategies (CPBP and CBP) opted for AVLR valorization, a cost-benefit analysis was performed for a plant capacity processing 1 MTPH. A process flow diagrams for CPBP (butanol production) and CBP (lignin fractionation and butanol production) strategy at an industrial scale are shown in supplementary Figures (Fig. S12 and Fig. S13).

3.9.1. Cash flow and profitability assessment

The cost-benefit analysis of CPBP and CBP has revealed a distinct capital, operational and economic profile as summarized in Table 4. The detailed breakdown of DFC (TPDC, TPIC and CFC) and operational cost (raw materials, utilities, maintenance, labor, laboratory and other miscellaneous cost) involved in the CPBP and CBP are provided in the Table S4 and S5 respectively. Among the two different strategies opted for AVLR valorization, the CPBP for butanol production has demonstrated a lesser DFC ($1,212,325) and operational cost ($370,720 per year) than CBP (DFC- $2,203,127) and operational cost- $1,213,320 per year). The cost effectiveness of this CPBP strategy might be attributed by the integration of multiple steps (pretreatment, saccharification and fermentation) in a single reactor. For the economic modelling, the contributions of equity and loan were assumed to be 15% and 85% of the DFC with 5% interest rate. A straight-line depreciation was applied for a project life of 20 years with

5% discount rate and 20% tax on profits. The annual product capacity (CPBP- 338,803 kg and CBP- 1,212,176 kg) was calculated based on the product yield, assuming the plant process 1 MTPH of AVLR biomass and operates for 24 h a day over a span of 346 days in a year. The revenue estimated based on the unit price of butanol- $1.73 per kg and lignin- $1.0 per kg [Haigh et al., 2018; Industry ARC, 2025] revealed that CBP strategy generated a higher revenue ($1,574,528 per year) owing to the dual products i.e., lignin and butanol indicating the market stability as compared to CPBP strategy. After deducting the annual operational expenses from revenue, the EBITDA was estimated as $215,409 per year (CPBP) and $361,208 per year (CBP). About 5% interest were computed on the loan and the profit before tax was determined by deducting the depreciation, amortization and interest from EBITDA. The annual net profit in CPBP ($143,231) and CBP ($236,091) strategy was assessed by deducting the interest charges and taxes from EBITDA. Based on the annual operational expenses and product capacity, the unit production cost of butanol in CPBP ($1.09 per kg) and CBP ($2.44 per kg) strategy were comparable with the other reported studies using corn stover ($2.77 per kg), Japanese cooked rice ($1.24 per kg) and de-oiled rice bran ($ 1.43 per kg) as feedstock [48,92,98]. Then, the financial metrics such as NPV, IRR and payback period was estimated to determine the economic feasibility of the plant. The NPV in CPBP ($572,650) and CBP ($739,089) strategy was found to be greater than zero indicating the financial worth of the project. And the economic feasibility was assessed by IRR (CPBP- ~10% and CBP- ~9%) and PBP (CPBP- 8.46 years and CBP- 9.33 years) for a project life of 20 years. Similarly, Ozturk et al. [48] investigated the cost-benefit analysis of butanol production from cooked rice using two-step fermentation, where the IRR and pay back period was estimated to be around 13% and 8 years.

Overall, CPBP strategy was found to be suitable for the plant setup preferring low capital and operational cost with simple unit operations. While, the CBP strategy with dual products has a

higher revenue and net profit. Therefore, strategy for AVLR valorization might be chosen based on the market demand of the product, availability of the capital cost, operational capacity, and desired PBP. Further, optimization of the production and use of comprehensive experimental dataset could refine the cost benefit analysis.

3.9.2. Sensitivity analysis

In order to avoid the financial risk and resolve the uncertainty in plant feasibility, sensitivity analysis of NPV against the various market conditions such as discount rate (2 to 8%), project life (15 to 25 years) and income tax (15 to 25%) was performed. From the Fig. 9(a and b), it was evident that the NPV for the base scenario (5% discount rate, 20 years of project life and 20% income tax) was estimated at 0.57 million dollars and 0.73 million dollars for CPBP and CBP strategy respectively. An increase in the project life has significantly increased the NPV for CPBP and CBP by 1.40-fold and 1.53-fold respectively. Whereas, a reverse trend (decrease in NPV) was observed when the discount rate was increased to 8% from the base scenario. The fluctuations in the income tax have a slight fold change in NPV, indicating its negligible role in influencing the process economics. Therefore, the sensitivity analysis implies that the project life (operational) and discount rate (market factor) are critical parameters in assessing the economic performance of these two different strategies.

4. Conclusion

This study offers insights into the adaption of ALE strategy for enriching the microbial symbionts from termite gut using various LCB for the establishment of microbial consortium. Upon screening the consortia, ETC-3 was found to be potent consortium with highest substrate degradation percentage and specific enzyme activities. In addition, the enrichment has significantly altered the microbial population in ETC-3 as compared to the native gut microbiome. A concoction of microbes with diverse lignocellulolytic enzyme production and hydrolysis potential are identified in different taxa of ETC-3. Further,

microbial consortium (ETC-3) mediated CPBP and CBP are identified as an economically feasible strategies for the valorization of AVLR biomass into butanol and value-added compound (lignin) as determined by cost-benefit analysis. Therefore, ETC-3 constitutes a pool of several lignocellulose degraders that are developed by the utmost adaptability of termite gut microbes upon sequential enrichment with AVLR could serve as potent microbial consortium for the integrating the unit operations in LCB-based biorefinery.

Credit Author Statement

Gunasekaran Rajeswari: Data curation, Formal analysis, Investigation, Methodology, Writing – original draft, Writing – review & editing, Visualization. **Vinod Kumar**: Conceptualization, Methodology, Supervision, Validation, Writing – review & editing. **Samuel Jacob**: Conceptualization, Methodology, Project administration, Supervision, Validation, Writing – review & editing.

Declarations

Ethical approval

Not applicable.

Competing interests

The authors declare that there is no competing interest associated with this manuscript.

Funding

Not applicable

Availably of data and materials

The 16S rRNA and ITS raw sequence reads of the termite microbiome and ETC-3 were submitted to the NCBI, with the accession numbers provided under the Bioproject PRJNA1182483.

Acknowledgements

The authors would like to acknowledge the Directorate of Research, SRM Institute of Science and Technology, Kattankulathur, for the financial support of their lignocellulosic research through the Selective Excellence Research Initiative scheme. The authors also acknowledge the Department of Biotechnology, School of Bioengineering, SRM Institute of Science and Technology for the financial support provided for the research as well as infrastructure to carry out the research work and Interdisciplinary Institute of Indian System of Medicine (IIISM),

Nanotechnology Research Centre (NRC), SRM Central Instrumentation Facility (SCIF) for providing the instrumental support.

Authors' information

Gunasekaran Rajeswari and Samuel Jacob

Department of Biotechnology, School of Bioengineering, College of Engineering and Technology, Faculty of Engineering and Technology, SRM Institute of Science and Technology, SRM Nagar, Chengalpattu District, Kattankulathur-603203, Tamil Nadu, India

Vinod Kumar

School of Water, Energy and Environment, Cranfield University, Cranfield, MK43 0AL, UK.

Department of Biotechnology, School of Bioengineering, College of Engineering and Technology, Faculty of Engineering and Technology, SRM Institute of Science and Technology, SRM Nagar, Chengalpattu District, Kattankulathur-603203, Tamil Nadu, India

Corresponding author

Correspondence to Samuel Jacob

References

[1] X. Liu, Y. Jiang, C. Qin, S. Yang, X. Song, S. Wang, K. Li, Enzyme-assisted mechanical grinding for cellulose nanofibers from bagasse: Energy consumption and nanofiber characteristics, Cellulose. 25 (2018) 7065 – 7078. https://doi.org/10.1007/s10570-018-2071-1.

[2] O.B. Chukwuma, M. Rafatullah, H.A. Tajarudin, N. Ismail, 2020. Lignocellulolytic enzymes in biotechnological and industrial processes: A review. Sustainability. 12, 7282. https://doi.org/10.3390/su12187282.

[3] R.S. Abolore, S. Jaiswal, A.K. Jaiswal, 2024. Green and sustainable pretreatment methods for cellulose extraction from lignocellulosic biomass and its applications: A review. Carbohydr. Polym. Technol. Appl. 7, 100396. https://doi.org/10.1016/j.carpta.2023.100396.

[4] M. Raud, T. Kikas, O. Sippula, N.J. Shurpali, Potentials and challenges in lignocellulosic biofuel production technology, Renew. Sustain. Energy Rev. 111 (2019) 44 – 56. https://doi.org/10.1016/j.rser.2019.05.020.

[5] K.N. Yogalakshmi, M.T.M. Usman, S. Kavitha, S. Sachdeva, S. Thakur, A.S. Kumar, B.J. Rajesh, 2023. Lignocellulosic biorefinery technologies: A perception into recent advances in biomass fractionation, biorefineries, economic hurdles and market outlook. Fermentation. 9, 238. https://doi.org/10.3390/fermentation9030238.

[6] A. Althuri, S. Venkata Mohan, 2020. Sequential and consolidated bioprocesxsing of biogenic municipal solid waste: A strategic pairing of thermophilic anaerobe and mesophilic microaerobe for ethanol production. Bioresour. Technol. 308, 123260. https://doi.org/10.1016/j.biortech.2020.123260.

[7] R.R. Singhania, A.K. Patel, A. Singh, D. Haldar, S. Soam, C.-W. Chen, M.-L. Tsai, C.-D. Dong, 2022. Consolidated bioprocessing of lignocellulosic biomass: technological advances and challenges. Bioresour. Technol. 354, 127153. https://doi.org/10.1016/j.biortech.2022.127153.

[8] M.J. de Lima Brossi, D.J. Jiménez, L. Cortes-Tolalpa, J.D. van Elsas, Soil-derived microbial consortia enriched with different plant biomass reveal distinct players acting in lignocellulose degradation, Microb. Ecol. 71 (2016) 616 – 627. https://doi.org/10.1007/s00248-015-0683-7.

[9] M. Marynowska, X. Goux, D. Sillam-Dussès, C. Rouland-Lefevre, R. Halder, P. Wilmes, P. Gawron, Y. Roisin, P. Delfosse, M. Calusinska, Compositional and functional characterisation of biomass-degrading microbial communities in guts of plant fibre- and soil-feeding higher termites, Microbiome. 8 (2020) 1 – 18. https://doi.org/10.1186/s40168-020-00872-3.

[10] G. Rajeswari, S. Jacob, A.K. Chandel, V. Kumar, 2021. Unlocking the potential of insect and ruminant host symbionts for recycling of lignocellulosic carbon with a biorefinery approach: A review. Microb. Cell Fact. 20, 107. https://doi.org/10.1186/s12934-021-01597-0.

[11] H. Konig, L. Li, J. Frohlich, The cellulolytic system of the termite gut, Appl. Microbiol. Biotechnol. 97 (2013) 7943 – 7962. https://doi.org/10.1007/s00253-013-5119-z.

[12] A. Brune, Symbiotic digestion of lignocellulose in termite guts, Nat. Rev. Microbiol. 12 (2014) 168 – 180. https://doi.org/10.1038/nrmicro3182.

[13] P. Eggleton, An introduction of termites: biology, taxonomy, and functional morphology, in: D.E. Bignell, Y. Roisin, N. Lo (Eds.), Biology of termites: A moderns synthesis, Springer Dordcreht Heidelberg, New York, 2011, pp. 1 - 26.

[14] S. Xie, R. Syrenne, S. Sun, J.S. Yuan, Exploration of natural biomass utilization systems (NBUS) for advanced biofuel — from systems biology to synthetic design, Curr. Opin. Biotechnol. 27 (2014) 195 – 203. https://doi.org/10.1016/j.copbio.2014.02.007.

[15] A. Ferbiyanto, I. Rusmana, R. Raffiudin, Characterization and identification of cellulolytic bacteria from gut of worker *Macrotermes gilvus*, HAYATI J. Biosci. 22 (2015) 197 – 200. https://doi.org/10.1016/j.hjb.2015.07.001.

[16] S.S. Ali, J. Wu, R. Xie, F. Zhou, J. Sun, M. Huang, 2017. Screening and characterizing of xylanolytic and xylose-fermenting yeasts isolated from the wood-feeding termite, *Reticulitermes chinensis*. PLoS One. 12, e0181141. https://doi.org/10.1371/journal.pone.0181141.

[17] L.M. Varghese, S. Agrawal, D. Sharma, R.P. Mandhan, R. Mahajan, Cost-effective screening and isolation of xylano-cellulolytic positive microbes from termite gut and termitarium, 3 Biotech. 7 (2017) 1 – 7. https://doi.org/10.1007/s13205-017-0733-6.

[18] A. Lazuka, L. Auer, M. O'Donohue, G. Hernandez-Raquet, 2018. Anaerobic lignocellulolytic microbial consortium derived from termite gut: enrichment, lignocellulose degradation and community dynamics. Biotechnol. Biofuels. 11, 248. https://doi.org/10.1186/s13068-018-1282-x.

[19] T.E. Sandberg, M.J. Salazar, L.L. Weng, B.O. Palsson, A.M. Feist, The emergence of adaptive laboratory evolution as an efficient tool for biological discovery and industrial biotechnology, Metab. Eng. 56 (2019) 1 – 16. https://doi.org/10.1016/j.ymben.2019.08.004.

[20] S. Lee, P. Kim, Current status and applications of adaptive laboratory evolution in industrial microorganisms, J. Microbiol. Biotechnol. 30 (2020) 793 – 803. https://doi.org/10.4014/jmb.2003.03072.

[21] M. Dragosits, D. Mattanovich, 2013. Adaptive laboratory evolution – Principles and applications for biotechnology. Microb. Cell Fact. 12, 64. https://doi.org/10.1186/1475-2859-12-64.

[22] G. Wang, Q. Li, Z. Zhang, X. Yin, B. Wang, X. Yang, 2023. Recent Progress in Adaptive Laboratory Evolution of Industrial Microorganisms. J. Ind. Microbiol. Biotechnol. 50, kuac023. https://doi.org/10.1093/jimb/kuac023.

[23] D.J. Hellen-Sathya, A.M. Turakhia, M.A. Kumar, N. Balaji, S. Selvanaveen, G. Vinodhini, M. Seenuvasan, Bioethanol from saccharificed lignocellulosic rich Aloe vera rinds using *Saccharomyces Cerevisiae* MTCC 4779, Energy sources, Part A: Recovery, Utilization, and Environmental effects. 39 (2017) 1347 – 1352. https://doi.org/10.1080/15567036.2017.1328004.

[24] G. Rajeswari, S. Jacob, 2021. Saccharolysis of laccase delignified *Aloe vera* leaf rind and fermentation through free and immobilized yeast for ethanol production. J. Food Process Eng. 44, e13514. https://doi.org/10.1111/jfpe.13514.

[25] G. Rajeswari, S. Jacob, Co-fermentation of lactic acid and acetone-butanol-ethanol (ABE) from the deep eutectic solvent–pretreated Aloe vera leaf rind through sequential valorization of holocellulose, Biomass Conv. Bioref. 14 (2024) 28429 – 28447. https://doi.org/10.1007/s13399-022-03688-3.

[26] M.B. Grieco, F.A.C. Lopes, L.S. Oliveira, D.A. Tschoeke, C.C. Popov, C.C. Thompson, L.C. Goncalves, R. Constantino, O.B. Martins, R.H. Kruger, W. de Souza, F.L. Thompson, Metagenomic analysis of the whole gut microbiota in Brazilian Termitidae termites *Cornitermes cumulans*, *Cyrilliotermes strictinasus*, *Syntermes dirus*, *Nasutitermes jaraguae*, *Nasutitermes aquilinus*, *Grigiotermes bequaerti*, and *Orthognathotermes mirim*, Curr. Microbiol. 76 (2019) 687 – 697. https://doi.org/10.1007/s00284-019-01662-3.

[27] F. Manzoor, M.S. Akhtar, Morphometric analysis of population samples of soldier caste of *Odontotermes obesus* (Rambur) (Isoptera, Termitidae, Macrotermitinae), Anim. Biodiverse Conserv. 29 (2006) 91 – 107. https://doi.org/10.32800/abc.2006.29.0091.

[28] Bhanupriya, S. Mukherjee, N. Kakkar, S.K. Gupta, Identification and phylogenetic analysis of various termite species distributed across southern Haryana, India, J. Threat. Taxa. 15 (2023) 23382 – 23396. https://doi.org/10.11609/jott.8168.15.6.23382-23396.

[29] Y.M. Chew, S. Lye, M. Md Salleh, A. Yahya, 16S rRNA metagenomic analysis of the symbiotic community structures of bacteria in foregut, midgut, and hindgut of the wood-feeding termite *Bulbitermes* sp, Symbiosis. 76 (2018) 187 – 197. https://doi.org/10.1007/s13199-018-0544-5.

[30] R.H. Santana, E.C.P. Catão, F.A.C. Lopes, R. Constantino, C.C. Barreto, R.H. Krüger, The gut microbiota of workers of the litter-feeding termite *Syntermes wheeleri* (Termitidae: Syntermitinae): Archaeal, bacterial, and fungal communities, Microb. Ecol. 70 (2015) 545 –556. https://doi.org/10.1007/s00248-015-0581-z.

[31] S. Vikram, J.D. Arneodo, J. Calcagno, M. Ortiz, M.L. Mon, C. Etcheverry, D.A. Cowan, P. Talia, 2021. Diversity structure of the microbial communities in the guts of four neotropical termite species. PeerJ. 9, e10959. https://doi.org/10.7717/peerj.10959.

[32] Z. Chen, X. Bai, A. Lusi, C. Wan, High-solid lignocellulose processing enabled by natural deep eutectic solvent for lignin extraction and industrially relevant production of renewable chemicals, ACS Sustain. Chem. Eng. 6 (2018) 12205 – 12216. https://doi.org/10.1021/acssuschemeng.8b02541.

[33] D.M. Updegraf, Semimicro determination of cellulose in biological materials, Anal. Biochem. 32 (1969) 420 – 424. https://doi.org/10.1016/S0003-2697(69)80009-6.

[34] J.A. Marlett, S.C. Lee, Dietary fiber, lignocellulose and hemicellulose contents of selected foods determined by modified and unmodified van soest procedures, J. Food Sci. 45 (1980) 1688 – 1893. https://doi.org/10.1111/j.1365-2621.1980.tb07590.x.

[35] A. Sluiter, B. Hames, R. Ruiz, C. Scarlata, J. Sluiter, D. Templeton, D. Crocker, Determination of structural carbohydrates and lignin in biomass, Laboratory analytical procedure, 2008, pp. 1 - 16.

[36] V.L. Papinutti, L.A. Diorio, F. Forchiassin, Production of laccase and manganese peroxidase by *Fomes sclerodermeus* grown on wheat bran, J. Ind. Microbiol. Biotechnol. 30 (2003) 157 – 160. https://doi.org/10.1007/s10295-003-0025-5.

[37] S.S. Bhattacharya, R. Banerjee, Laccase mediated biodegradation of 2,4-dichlorophenol using response surface methodology, Chemosphere. 73 (2008) 81 – 85. https://doi.org/10.1016/j.chemosphere.2008.05.005.

[38] M. Vrsanska, S. Voberkova, V. Langer, D. Palovcikova, A. Moulick, V. Adam, P. Kopel, 2016. Induction of laccase, lignin peroxidase and manganese peroxidase activities in white-rot fungi using copper complexes. Molecules. 21, 1553. https://doi.org/10.3390/molecules21111553.

[39] T.K. Ghose, V.S. Bisaria, Measurement of hemicellulase activities: Part I Xylanases, Pure Appl. Chem. 59 (1987) 1739 – 1751. https://doi.org/10.1351/pac198759121739.

[40] D.E. Eveleigh, M. Mandels, R. Andreotti, Roche, Measurement of saccharifying cellulase, Biotechnol. Biofuels. 2 (2009) 1 – 8. https://doi.org/10.1186/1754-6834-2-21.

[41] S. Sadasivam, A. Manickam, Biochemical methods, New Delhi, New age International, 1996.

[42] G.L. Miller, Use of dinitrosalicylic acid reagent for determination of reducing sugar, Anal. Chem. 31 (1959) 426 – 428. https://doi.org/10.1021/ac60147a030.

[43] G. Rajeswari, V. Kumar, S. Jacob, 2024. A concerted enzymatic de-structuring of lignocellulosic materials using a compost-derived microbial consortia favoring the consolidated pretreatment and bio-saccharification. Enzyme Microb. Technol. 174, 110393. https://doi.org/10.1016/j.enzmictec.2023.110393.

[44] P.J. Pham, R. Hernandez, W.T. French, B.G. Estill, A.H. Mondala, A spectrophotometric method for quantitative determination of xylose in fermentation medium, Biomass Bioenerg. 35 (2011) 2814 – 2821. https://doi.org/10.1016/j.biombioe.2011.03.006.

[45] M.A. Hossain, M.S. Rahaman, D. Yelle, H. Shang, Z. Sun, S. Renneckar, J. Dong, S. Tulaphol, N. Sathitsuksanoh, 2021. Effects of polyol-based deep eutectic solvents on the efficiency of rice straw enzymatic hydrolysis. Ind. Crop. Prod. 167, 113480. https://doi.org/10.1016/j.indcrop.2021.113480.

[46] L. Segal, J.J. Creely, A.E. Martin, C.M. Conrad, An empirical method for estimating the degree of crystallinity of native cellulose using the X-ray diffractometer, Text. Res. J. 29 (1959) 786 – 794. https://doi.org/10.1177/004051755902901003.

[47] Y. Zhu, B. Qi, X. Liang, J. Luo, Y. Wan, 2021. Comparison of corn stover pretreatments with lewis acid catalyzed choline chloride, glycerol and choline chloride-glycerol deep eutectic solvent. Polymers. 13, 1170. https://doi.org/10.3390/polym13071170.

[48] A.B. Ozturk, T. Arasoglu, J. Gulen, S. Cheng, N.K.N. Al-Shorgani, H. Habaki, R. Egashira, M.S. Kalil, W.M.W. Yusoff, J.S. Cross, Techno-economic analysis of a two-step fermentation process for bio-butanol production from cooked rice, Sustain. Energy Fuels. 5 (2021) 3705 –3718. https://doi.org/10.1039/D1SE00496D.

[49] Y.J. Liu, B. Li, Y. Feng, Q. Cui, 2020. Consolidated bio-saccharification: Leading lignocellulose bioconversion into the real world. Biotechnol. Adv. 40, 107535. https://doi.org/10.1016/j.biotechadv.2020.107535.

[50] M. Mavrommati, A. Daskalaki, S. Papanikolaou, G. Aggelis, 2022. Adaptive laboratory evolution principles and applications in industrial biotechnology. Biotechnol. Adv. 54, 107795. https://doi.org/10.1016/j.biotechadv.2021.107795.

[51] Y. Hongoh, L. Ekpornprasit, T. Inoue, S. Moriya, S. Trakulnaleamsai, M. Ohkuma, N. Noparatnaraporn, T. Kudo, Intracolony Variation of Bacterial Gut Microbiota among Castes and Ages in the Fungus-Growing Termite *Macrotermes gilvus*, Mol. Ecol. 15 (2005) 505 – 516. https://doi.org/10.1111/j.1365-294X.2005.02795.x.

[52] M.-I. Lucy, W.T.M. Anne, O. Ellie, L. Wilber, K. Martin, T. Grover, B. Hamadi, Bacterial diversity in intestinal tract of fungus-cultivating termite *Macrotermes michaelseni*, Afr. J. Biotechnol. 6 (2007) 658 – 667. https://doi.org/10.4314/ajb.v6i6.56873.

[53] E.D. Sonnenburg, H. Zheng, P. Joglekar, S.K. Higginbottom, S.J. Firbank, D.N. Bolam, J.L. Sonnenburg, Specificity of polysaccharide use in intestinal bacteroides species determines diet-induced microbiota alterations, Cell. 141 (2010) 1241 – 1252. https://doi.org/10.1016/j.cell.2010.05.005.

[54] N. Liu, X. Yan, M. Zhang, L. Xie, Q. Wang, Y. Huang, X. Zhou, S. Wang, Z. Zhou, Microbiome of fungus-growing termites: A new reservoir for lignocellulase genes, Appl. Environ. Microbiol. 77 (2011) 48 – 56. https://doi.org/10.1128/AEM.01521-10.

[55] Y. Kodama, T. Shimoyama, K. Watanabe, *Dysgonomonas oryzarvi sp.* nov., isolated from a microbial fuel cell, Int. J. Syst. Evol. Microbiol. 62 (2012) 3055 – 3059. https://doi.org/10.1099/ijs.0.039040-0.

[56] Y. Zhu, J. Li, H. Liu, H. Yang, S. Xin, F. Zhao, X. Zhang, Y. Tian, X. Lu, Phylogenetic analysis of the gut bacterial microflora of the fungus-growing termite *Macrotermes barneyi*, Afr. J. Microbiol. Res. 6 (2012) 2071 – 2078. https://doi.org/10.5897/AJMR11.1345.

[57] N. Zhu, J. Yang, L. Ji, J. Liu, Y. Yang, H. Yuan, 2016. Metagenomic and metaproteomic analyses of a corn stover-adapted microbial consortium EMSD5 reveal its taxonomic and enzymatic basis for degrading lignocellulose. Biotechnol. Biofuels. 9, 243. https://doi.org/10.1186/s13068-016-0658-z.

[58] M. Le Roes-Hill, J. Rohland, S. Burton, Actinobacteria isolated from termite guts as a source of novel oxidative enzymes, Antonie van Leeuwenhoek. 100 (2011) 589 – 605. https://doi.org/10.1007/s10482-011-9614-x.

[59] T.D.H. Bugg, M. Ahmad, E.M. Hardiman, R. Rahmanpour, Pathways for degradation of lignin in bacteria and fungi, Nat. Prod. Rep. 28 (2011) 1883 – 1896. https://doi.org/10.1039/C1NP00042J.

[60] T. Köhler, C. Dietrich, R.H. Scheffrahn, A. Brune, High-resolution analysis of gut environment and bacterial microbiota reveals functional compartmentation of the gut in wood-feeding higher termites (*Nasutitermes spp.*), Appl. Environ. Microbiol. 78 (2012) 4691 – 4701. https://doi.org/10.1128/AEM.00683-12.

[61] A. Mikaelyan, C. Dietrich, T. Köhler, M. Poulsen, D. Sillam-Dussès, A. Brune, Diet is the primary determinant of bacterial community structure in the guts of higher termites, Mol. Ecol. 24 (2015) 5284 – 5295. https://doi.org/10.1111/mec.13376.

[62] K. Rossmassler, C. Dietrich, C. Thompson, A. Mikaelyan, J.O. Nonoh, R.H. Scheffrahn, D. Sillam-Dussès, A. Brune, 2015. Metagenomic analysis of the microbiota

in the highly compartmented hindguts of six wood- or soil-feeding higher termites. Microbiome. 3, 56. https://doi.org/10.1186/s40168-015-0118-1.

[63] L. Su, L. Yang, S. Huang, X. Su, Y. Li, F. Wang, E. Wang, N. Kang, J. Xu, A. Song, 2015. Comparative gut microbiomes of four species representing the higher and the lower termites. J. Insect Sci. 16, 97. https://doi.org/10.1093/jisesa/iew081.

[64] N.R. Ballor, I. Paulsen, J.R. Leadbetter, Genomic analysis reveals multiple [FeFe] hydrogenases and hydrogen sensors encoded by *Treponemes* from the H_2-rich termite gut, Microb. Ecol. 63 (2015) 282 – 294. https://doi.org/10.1007/s00248-011-9922-8.

[65] A.A. Visser, V.I.D. Ros, Z.W. De Beer, A.J.M. Debets, E. Hartog, T.W. Kuyper, T. Laessoe, B. Slippers, D.K. Aanen, Levels of specificity of Xylaria species associated with fungus-growing termites: A phylogenetic approach, Mol. Ecol. 18 (2009) 553 – 567. https://doi.org/10.1111/j.1365-294X.2008.04036.x.

[66] J. Korb, H.M. Makonde, H.I. Boga, Z. Osiemo, R. Mwirichia, J.B. Stielow, M. Göker, H.-P. Klenk, 2013. Diversity of *Termitomyces* associated with fungus-farming termites assessed by cultural and culture-independent methods. PLoS One. 8, e56464. https://doi.org/10.1371/journal.pone.0056464.

[67] J. Rytioja, K. Hildén, J. Yuzon, A. Hatakka, R.P. de Vries, M.R. Mäkelä, Plant-polysaccharide-degrading enzymes from *Basidiomycetes*, Microbiol. Mol. Biol. Rev. 78 (2014) 614 – 649. https://doi.org/10.1128/MMBR.00035-14.

[68] J. Zhou, J. Duan, M. Gao, Y. Wang, X. Wang, K. Zhao, Diversity, roles, and biotechnological applications of symbiotic microorganisms in the gut of termite, Curr. Microbiol. 76 (2018) 755 – 761. https://doi.org/10.1007/s00284-018-1502-4.

[69] R.P. de Vries, R. Riley, A. Wiebenga, G. Aguilar-Osorio, S. Amillis, C.A. Uchima, G. Anderluh, M. Asadollahi, M. Askin, K. Barry, E. Battaglia, Ö. Bayram, T. Benocci,

S.A. Braus-Stromeyer, C. Caldana, D. Cánovas, G.C. Cerqueira, F. Chen, et al., 2017. Comparative genomics reveals high biological diversity and specific adaptations in the industrially and medically important fungal genus *Aspergillus*. Genome Biol. 18, 28. https://doi.org/10.1186/s13059-017-1151-0.

[70] N. Namnuch, A. Thammasittirong, S.N. Thammasittirong, Lignocellulose hydrolytic enzymes production by *Aspergillus flavus* KUB2 using submerged fermentation of sugarcane bagasse waste. Mycology. 12 (2020) 119 – 127. https://doi.org/10.1080/21501203.2020.1806938.

[71] V.K. Nathan, S.R. Kanthimathinathan, M.E. Rani, G. Rathinasamy, N.D. Kannan, Biobleaching of waste paper using lignolytic enzyme from *Fusarium equiseti* VKF2: A mangrove isolate, Cellulose. 25 (2018) 4179 – 4192. https://doi.org/10.1007/s10570-018-1834-z.

[72] J. Larsbrink, L.S. McKee, Bacteroidetes bacteria in the soil: Glycan acquisition, enzyme secretion, and gliding motility, Adv. Appl. Microbiol. 110 (2020) 63 – 98. https://doi.org/10.1016/bs.aambs.2019.11.001.

[73] P.V. Gavande, A. Basak, S. Sen, K. Lepcha, N. Murmu, V. Rai, D. Mazumdar, S.P. Saha, V. Das, S. Ghosh, 2021. Functional characterization of thermotolerant microbial consortium for lignocellulolytic enzymes with central role of *Firmicutes* in rice straw depolymerization. Sci. Rep. 11, 3032. https://doi.org/10.1038/s41598-021-82163-x.

[74] D.J. Jiménez, M.J. de Lima Brossi, J. Schückel, S.K. Kračun, W.G.T. Willats, J.D. van Elsas, Characterization of three plant biomass-degrading microbial consortia by metagenomics- and metasecretomics-based approaches, Appl. Microbiol. Biotechnol. 100 (2016) 10463 – 10477. https://doi.org/10.1007/s00253-016-7713-3.

[75] L. Cortes-Tolalpa, D.J. Jiménez, M.J. de Lima Brossi, J.F. Salles, J.D. van Elsas, Different inocula produce distinctive microbial consortia with similar lignocellulose

degradation capacity, Appl. Microbiol. Biotechnol. 100 (2016) 7713 – 7725. https://doi.org/10.1007/s00253-016-7516-6.

[76] B. Tsegaye, C. Balomajumder, P. Roy, Isolation and characterization of novel lignolytic, cellulolytic, and hemicellulolytic bacteria from wood-feeding termite *Cryptotermes brevis*, Int. Microbiol. 22 (2018) 29 – 39. https://doi.org/10.1007/s10123-018-0024-z.

[77] L. Dumond, L.P.Y. Lam, G. van Erven, M. Kabel, F. Mounet, J. Grima-Pettenati, Y. Tobimatsu, G. Hernandez-Raquet, Termite gut microbiota contribution to wheat straw delignification in anaerobic bioreactors, ACS Sustain. Chem. Eng. 9 (2021) 2191 – 2202. https://doi.org/10.1021/acssuschemeng.0c07817.

[78] P.S. Sadalage, M.A. Dar, A.R. Chavan, K.D. Pawar, Formulation of synthetic bacterial consortia and their evaluation by principal component analysis for lignocellulose rich biomass degradation, Renew. Energ. 148 (2019) 467 – 477. https://doi.org/10.1016/j.renene.2019.10.053.

[79] T.D.H. Bugg, M. Ahmad, E.M. Hardiman, R. Singh, The emerging role for bacteria in lignin degradation and bio-product formation, Curr. Opin. Biotechnol. 22 (2011) 394 – 400. https://doi.org/10.1016/j.copbio.2010.10.009.

[80] J.L. Blanchard, R.I. Munir, J. Schellenberg, B. Henrissat, T.J. Verbeke, R. Sparling, D.B. Levin, 2014. Comparative analysis of carbohydrate active enzymes in *Clostridium termitidis* CT1112 reveals complex carbohydrate degradation ability. PLoS One. 9, e104260. https://doi.org/10.1371/journal.pone.0104260.

[81] D.M. Ha-Tran, T.T.M. Nguyen, C.-C. Huang, 2021. *Clostridium thermocellum* as a promising source of genetic material for designer cellulosomes: An overview. Catalysts. 11, 996. https://doi.org/10.3390/catal11080996.

[82] P. Chen, L. Yan, S. Zhang, Z. Wu, S. Li, X. Yan, N. Wang, N. Liang, H. Li, Optimizing bioconversion of ferulic acid to vanillin by *Bacillus Subtilis* in the stirred packed reactor using box-behnken design and desirability function, Food Sci. Biotechnol. 26 (2017) 143 – 152. https://doi.org/10.1007/s10068-017-0019-0.

[83] D. Zhu, P. Zhang, C. Xie, W. Zhang, J. Sun, W.-J. Qian, B. Yang, 2017. Biodegradation of alkaline lignin by *Bacillus ligniniphilus* L1. Biotechnol. Biofuels. 10, 44. https://doi.org/10.1186/s13068-017-0735-y.

[84] J. Mei, X. Shen, L. Gang, H. Xu, F. Wu, L. Sheng, 2020. A novel lignin degradation bacteria-*Bacillus amyloliquefaciens* SL-7 used to degrade straw lignin efficiently. Bioresour. Technol. 310, 123445. https://doi.org/10.1016/j.biortech.2020.123445.

[85] Z. Holesova, M. Jakubkova, I. Zavadiakova, I. Zeman, L. Tomaska, J. Nosek, Gentisate and 3-oxoadipate pathways in the yeast *Candida parapsilosis*: Identification and functional analysis of the genes coding for 3-hydroxybenzoate 6-hydroxylase and 4-hydroxybenzoate 1-hydroxylase, Microbiology. 157 (2011) 2152 – 2163. https://doi.org/10.1099/mic.0.048215-0.

[86] S.S. Ali, R. Al-Tohamy, T.M. Mohamed, Y.A.G. Mahmoud, H.A. Ruiz, L. Sun, J. Sun, 2022. Could termites be hiding a goldmine of obscure yet promising yeasts for energy crisis solutions based on aromatic wastes? A critical state-of-the-art review. Biotechnol. Biofuels Bioprod. 15, 35. https://doi.org/10.1186/s13068-022-02131-z.

[87] Q. Song, B. Wang, Ye. Han, Z . Zhou, 2022. Metagenomics reveals the diversity and taxonomy of carbohydrate-active enzymes and antibiotic resistance genes in Suancai bacterial communities. Genes. 13, 773. https://doi.org/10.3390/genes13050773.

[88] M. Ilmén, R. den Haan, E. Brevnova, J. McBride, E. Wiswall, A. Froehlich, A. Koivula, S.P. Voutilainen, M. Siika-aho, D.C. la Grange, N. Thorngren, S. Ahlgren, M. Mellon,

K. Deleault, V. Rajgarhia, W.H. van Zyl, M. Penttila, High level secretion of cellobiohydrolases by *Saccharomyces cerevisiae*, Biotechnol. Biofuels. 4 (2011) 1 – 15. https://doi.org/10.1186/1754-6834-4-30.

[89] W. Zhang, X. Ren, L. Wang, 2021. Screening and comparison of lignin degradation microbial consortia from wooden antiques. Molecules. 26, 2862. https://doi.org/10.3390/molecules26102862.

[90] B. Tsegaye, C. Balomajumder, P. Roy, Biodegradation of wheat straw by *Ochrobactrum oryzae* BMP03 and *Bacillus sp.* BMP01 bacteria to enhance biofuel production by increasing total reducing sugars yield, Environ. Sci. Pollut. Res. Int. 25 (2018) 30585 – 30596. https://doi.org/10.1007/s11356-018-3056-1.

[91] B. Tsegaye, C. Balomajumder, P. Roy, 2018. Biodelignification and hydrolysis of rice straw by novel bacteria isolated from wood feeding termite. 3 Biotech. 8, 447. https://doi.org/10.1007/s13205-018-1471-0.

[92] N.K.N. Al-Shorgani, A.I. Al-Tabib, A. Kadier, M.F. Zanil, K.M. Lee, M.S. Kalil, 2019. Continuous butanol fermentation of dilute acid-pretreated de-oiled rice bran by *Clostridium acetobutylicum* YM1. Sci. Rep. 9, 4622. https://doi.org/10.1038/s41598-019-40840-y.

[93] M. Yoshida, Y. Liu, S. Uchida, K. Kawarada, Y. Ukagami, H. Ichinose, S. Kaneko, K . Fukuda, Effects of cellulose crystallinity, hemicellulose, and lignin on the enzymatic hydrolysis of *Miscanthus sinensis* to monosaccharides, Biosci. Biotechnol. Biochem., 72 (2008) 805 –810. https://doi.org/10.1271/bbb.70689.

[94] R.C. Rajak, R. Banerjee, 2020. An innovative approach of mixed enzymatic venture for 2G ethanol production from lignocellulosic feedstock. Energy Convers. Manag. 207, 112504. https://doi.org/10.1016/j.enconman.2020.112504.

[95] L. Sun, P. Varanasi, F. Yang, D. Loqué, B.A. Simmons, S. Singh, Rapid determination of syringyl: guaiacyl ratios using FT-Raman spectroscopy, Biotechnol. Bioeng. 109 (2011) 647 –656. http://dx.doi.org/10.1002/bit.24348.

[96] F. Lionetto, R.D. Sole, D. Cannoletta, G. Vasapollo, A. Maffezzoli, Monitoring wood degradation during weathering by cellulose crystallinity, Materials. 5 (2012) 1910 – 1922. https://doi.org/10.3390/ma5101910.

[97] Z. Shi, G. Xu, J. Deng, M. Dong, V. Murugadoss, C. Liu, Q. Shao, S. Wu, Z. Guo, Structural characterization of lignin from *D. sinicus* by FTIR and NMR techniques, Green Chem. Lett. Rev. 12 (2019) 235 – 243. https://doi.org/10.1080/17518253.2019.1627428.

[98] A. Roussos, N. Misailidis, A. Koulouris, F. Zimbardi, D. Petrides, 2019. A feasibility study of cellulosic isobutanol production—process simulation and economic analysis. Processes. 7, 667. https://doi.org/10.3390/pr7100667.

Table 1 Specific activity of extracellular lignocellulolytic enzymes determined in various consortia (ETC-1 to ETC-6)

Lignocellulolytic enzymes		Specific enzyme activity (IU/mg of protein)					
		ETC-1	**ETC-2**	**ETC-3**	**ETC-4**	**ETC-5**	**ETC-6**
Ligninolytic enzyme	**Laccase**	29.78 ± 1.78	23.25 ± 0.70	33.23 ± 1.39	26.13 ± 1.41	N.D	
	LiP	2.42 ± 0.26	3.29 ± 0.20	7.95 ± 0.62	3.52 ± 0.62	N.D	
	MnP	5.37 ± 0.33	1.99 ± 0.14	7.52 ± 0.76	4.16 ± 0.73	N.D	
Hemicellulolytic enzyme	**Xylanase**	0.53 ± 0.02	0.28 ± 0.11	1.52 ± 0.26	0.77 ± 0.37	N.D	
Cellulolytic enzyme	**Endoglucanase**	6.67 ± 0.16	4.49 ± 0.90	15.30 ± 0.77	8.61 ± 0.40	24.19 ± 1.47	17.08 ± 1.38
	Total cellulase	1.32 ± 0.07	1.04 ± 0.17	1.94 ± 0.26	1.45 ± 0.35	3.20 ± 0.55	2.34 ± 0.32

N.D-Negligible deviation

Table 2 Fermentable sugar monomers yield after CPBP and CBP of AVLR biomass

Process strategies	CPBP	CBP
Xylose yield (mg/g)	121.65 ± 5.54	148.71 ± 6.28
Arabinose yield (mg/g)	36.74 ± 4.67	44.96 ± 11.98
Glucose yield (mg/g)	212.77 ± 5.70	305.55 ± 16.54
Saccharification percentage (%, w/w) (based on glucose yield)	49.82 ± 1.77	63.75 ± 2.54

Table 3 Yield and productivity of ABE obtained after CPBP and CBP of AVLR biomass

Process strategies	**CPBP**				**CBP**			
Parameters	**Acetone**	**Butanol**	**Ethanol**	**Total ABE**	**Acetone**	**Butanol**	**Ethanol**	**Total ABE**
Product yield (g/L)	0.97 ± 0.15	5.45 ± 0.37	0.35 ± 0.03	6.77 ± 0.55	2.18 ± 0.08	7.97 ± 0.40	0.36 ± 0.02	10.51 ± 0.50
Product yield coefficient Yp/s (g/g of glucose)	0.05 ± N.D	0.29 ± 0.02	0.02 ± N.D	0.36 ± 0.03	0.09 ± 0.01	0.32 ± 0.02	0.01 ± N.D	0.42 ± 0.03
Product productivity (g/L.h)	0.01 ± N.D	0.07 ± N.D	0.004 ± N.D	0.08 ± N.D	0.02 ± N.D	0.11 ± N.D	0.005 ± N.D	0.13 ± N.D
Fermentation efficiency (%)	16.03 ± 1.50	70.57 ± 5.80	3.63 ± 0.25	28.96 ± 7.55	27.08 ± 1.80	77.56 ± 3.00	2.85 ± 0.15	33.81 ± 4.95

N.D- negligible deviation

Table 4 Cash flow and profitability assessment of CPBP and CBP strategy

Process strategies	CPBP	CBP
DFC ($)	1,212,324.76	2,203,127.02
Equity ($)	181,848.72	330,469.05
Loan ($)	1,030,476.05	1,872,657.95
Discount rate (%)	5	5
Interest rate (%)	5	5
Operating cost ($ per year)	370,720.49	1,213,320.06
Product capacity (kg per year)	338,803.20	1,212,176.00
Revenue ($ per year)	586,129.54	1,574,528.00
EBITDA ($ per year)	215,409.00	361,208.00
Depreciation and amortization ($ per year)	60,616.24	110,156.35
Interest charges ($ per year)	51,524.00	93,633.00
Profit before tax ($ per year)	103,269.00	157,418.00
Income tax (20%) ($ per year)	20,653.80	31,483.67
Net profit ($ per year)	143,231.00	236,091.00
Project life (year)	20	20
NPV ($)	572,650.00	739,089.00
IRR (%)	~10	~8.69
PBP (year)	8.46	9.33
Unit production cost of butanol ($/kg)	1.09	2.44
Unit production cost of lignin ($/kg)	N.A	1.70

N.A. – Not applicable

Figure captions

Fig. 1. Morphology of different castes of termites (a), isolation of termite gut (b) and the various segments of the isolated gut (c) sample

Fig. 2. A schematic representation of ALE strategy for enriching the microbial consortia derived from termite gut

Fig. 3. Relative abundance of bacterial (a) and fungal (b) population in native termite gut microbiome at phylum, family and genus level

Fig. 4. Screening of enriched microbial consortia based on degradation of structural components (a); fermentable xylose (b), arabinose (c) and glucose (d) yield; PCA (e) and spearman correlation heat map (f and g) derived from termite gut. (NA- Not applicable)

Fig. 5. Chord diagram representing the comparison of relative abundance of microbial communities in native termite gut and ETC-3: (a) and (b) represents the bacterial population at phylum and order level and (c) and (d) represents the fungal population at phylum and order level respectively.

Fig. 6. Pearson correlation matrix representing the influence of ETC-3 on AVLR cell wall components degradation, sugar yield and abundance of bacterial (a) and fungal (b) community. (C5 represents- Pentose sugar (Arabinose and xylose) and C6 sugar- Hexose sugar (Glucose)

Fig. 7. Degradation of structural cell wall components and fermentation profile of ABE production during CPBP (a and c) and CBP (b and d) of AVLR biomass respectively

Fig. 8. SEM (a), XRD (b) and FTIR (c) analysis of untreated and treated AVLR biomass under different process strategies

Fig. 9. Sensitivity analysis of NPV for different process strategies (a) CPBP and (b) CBP

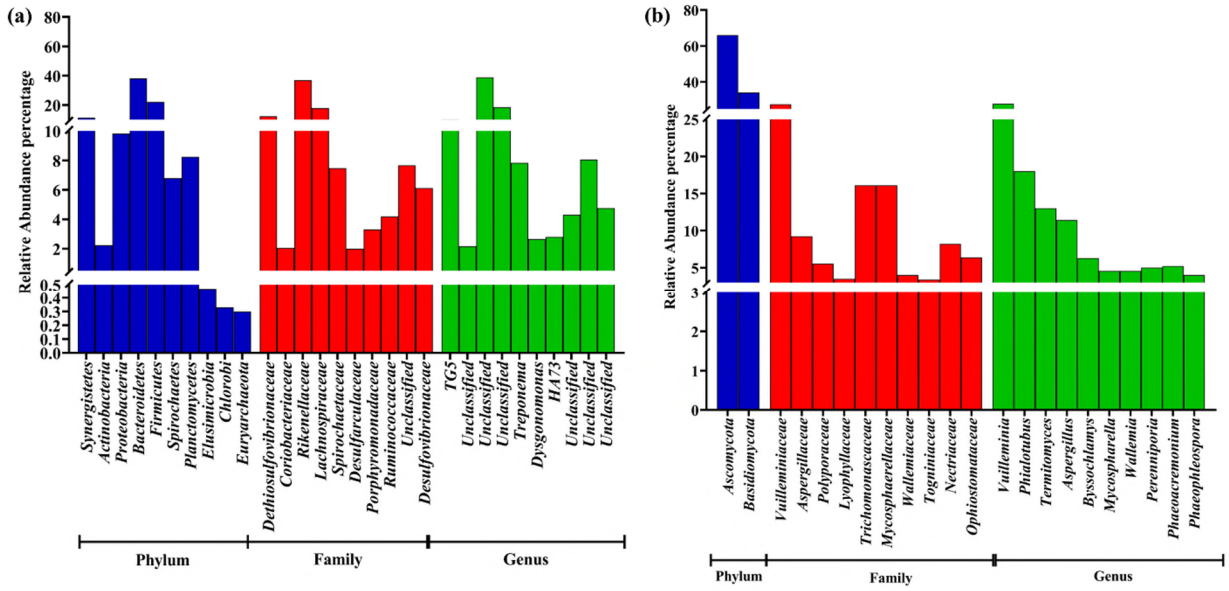


Fig. 3. Relative abundance of bacterial (a) and fungal (b) population in native termite gut microbiome at phylum, family and genus level

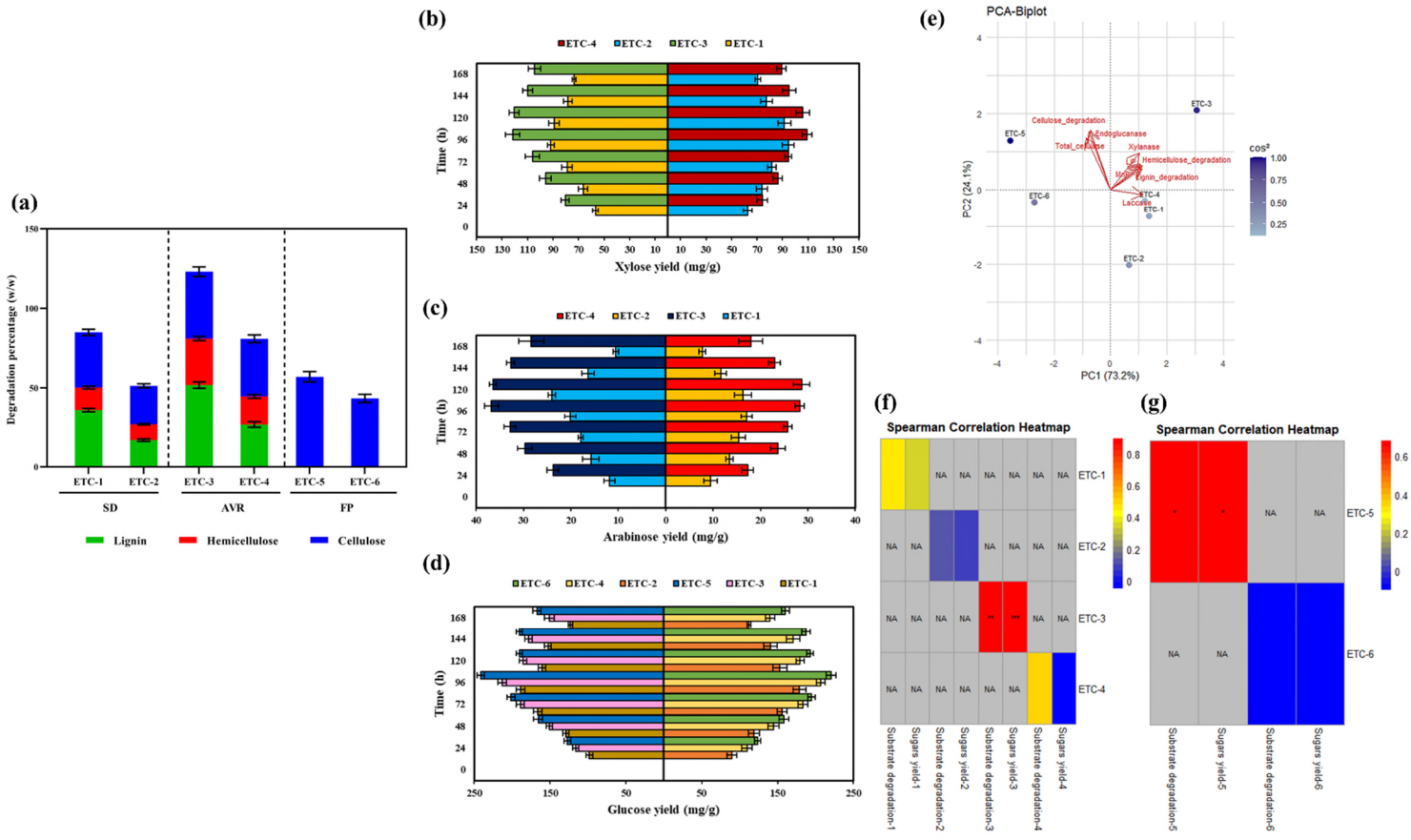


Fig. 4. Screening of enriched microbial consortia based on degradation of structural components (a); fermentable xylose (b), arabinose (c) and glucose (d) yield; PCA (e) and spearman correlation heat map (f and g) derived from termite gut. (NA- Not applicable)

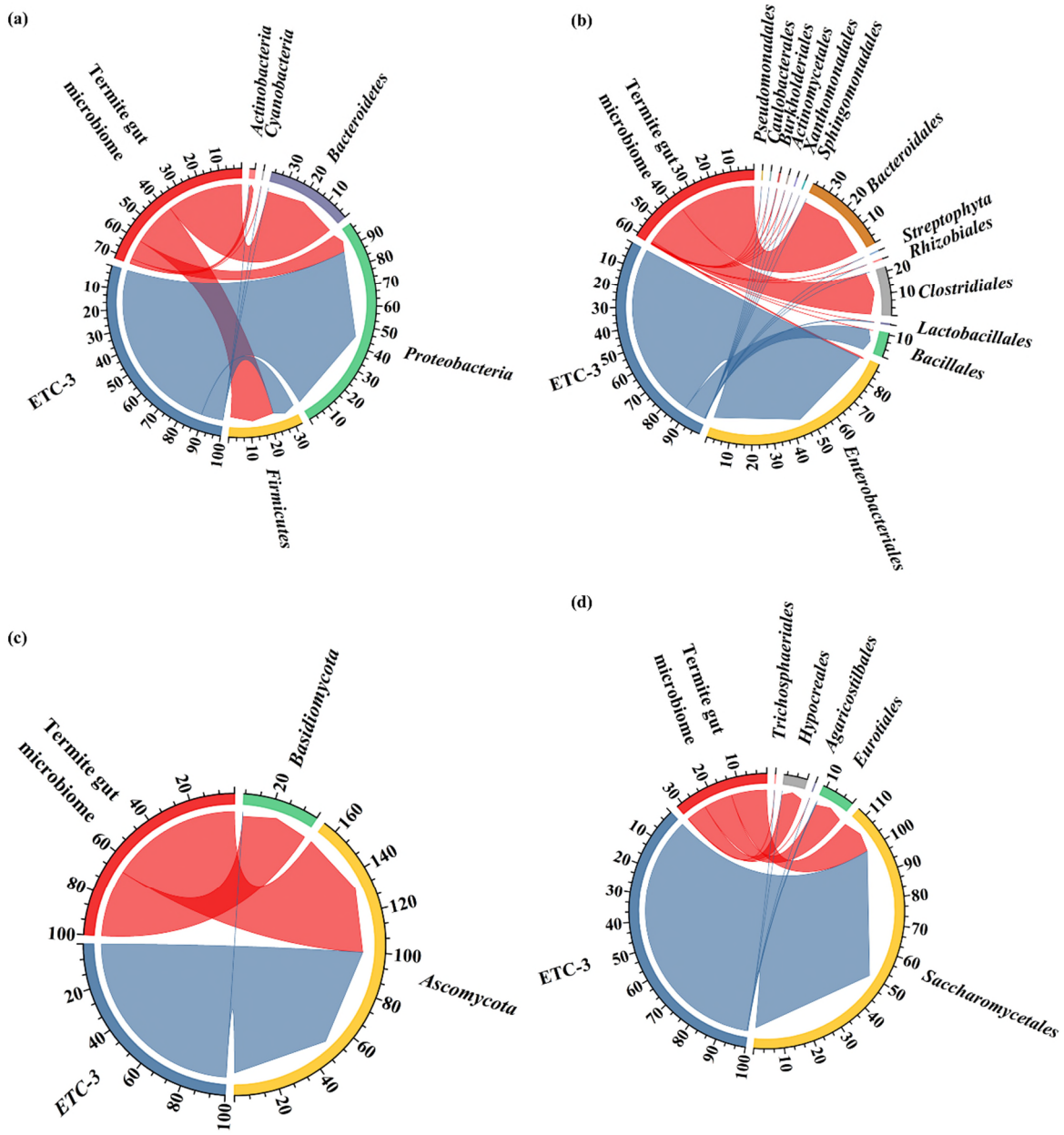


Fig. 5. Chord diagram representing the comparison of relative abundance of microbial communities in native termite gut and ETC-3: (a) and (b) represents the bacterial population at phylum and order level and (c) and (d) represents the fungal population at phylum and order level respectively.

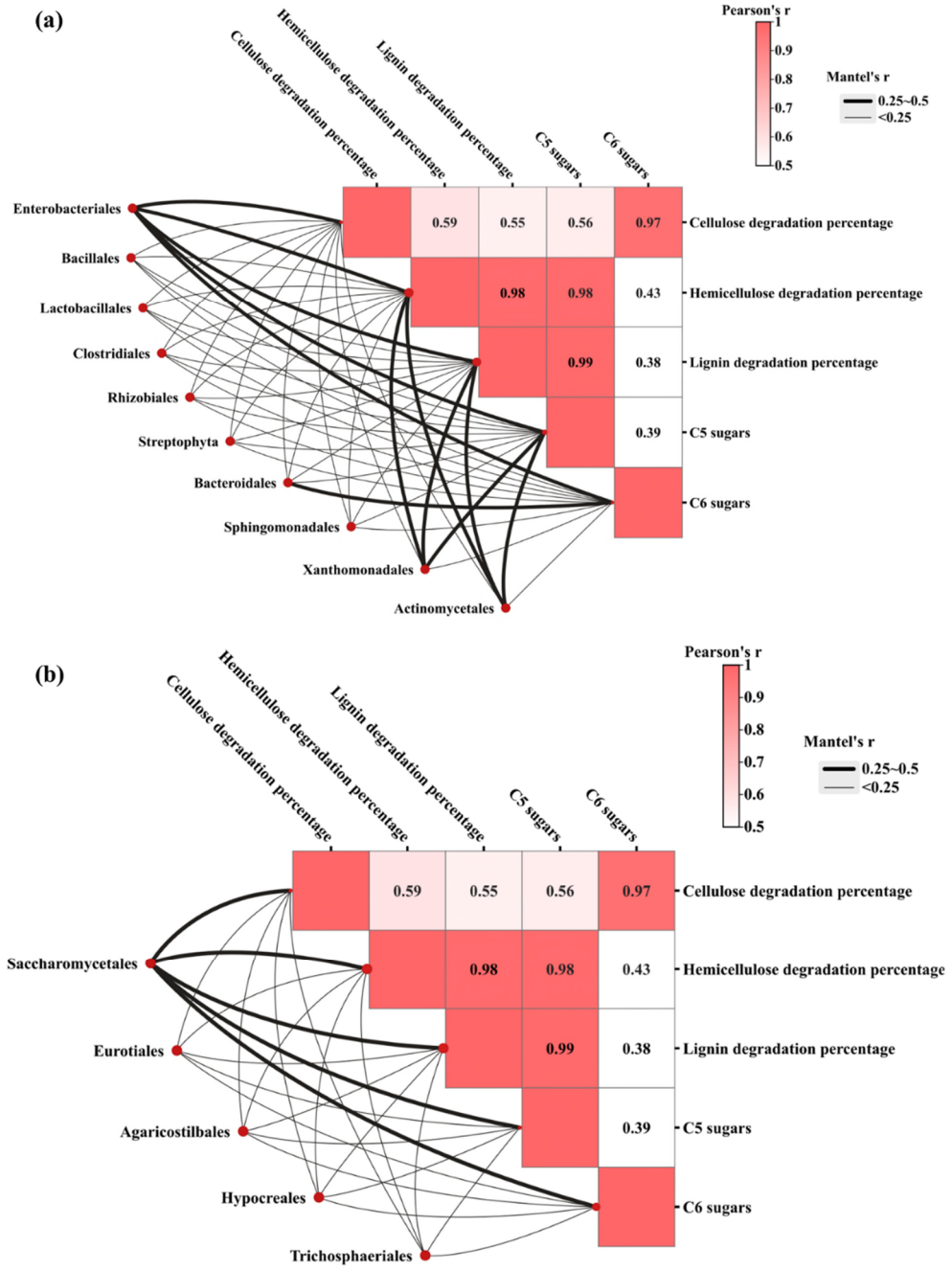


Fig. 6. Pearson correlation matrix representing the influence of ETC-3 on AVLR cell wall components degradation, sugar yield and abundance of bacterial (a) and fungal (b) community. (C5 represents- Pentose sugar (Arabinose and xylose) and C6 sugar- Hexose sugar (Glucose)

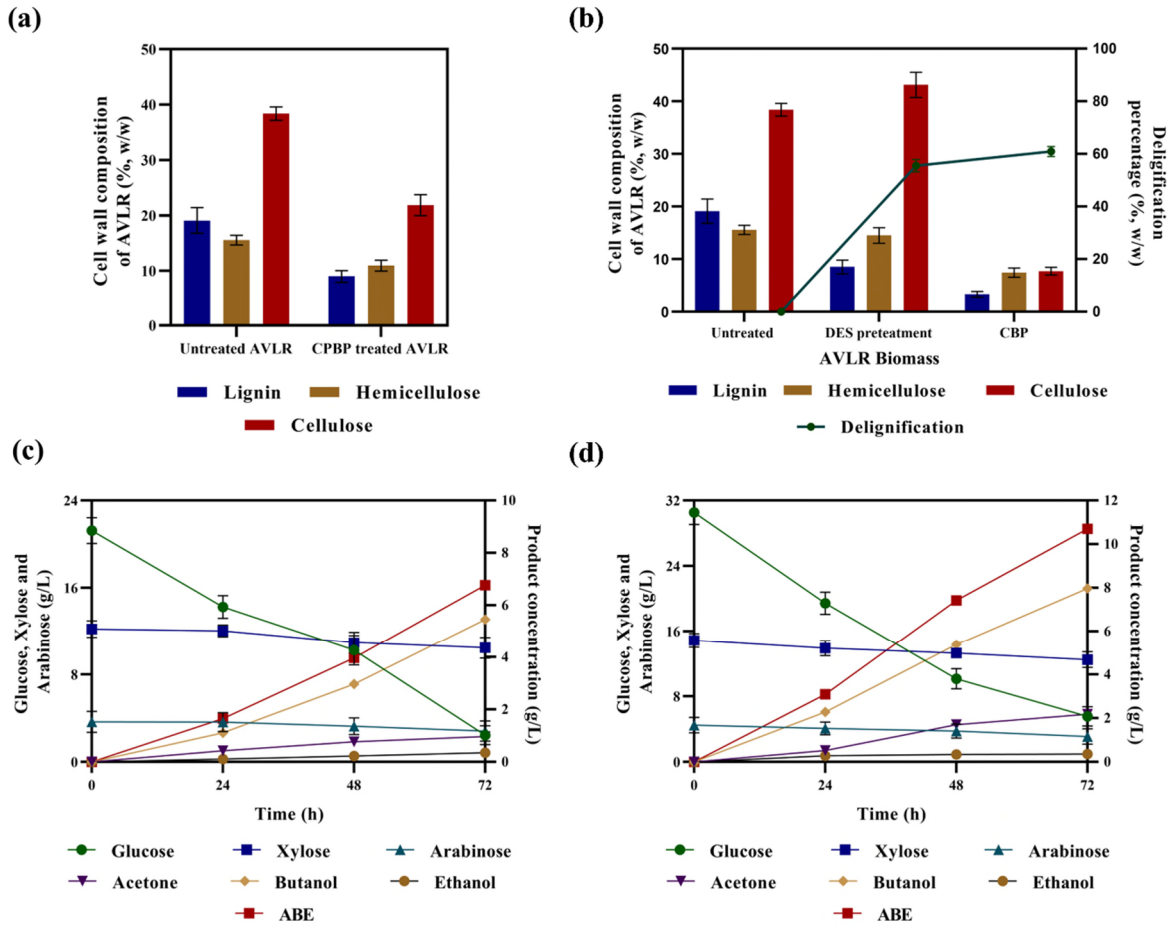


Fig. 7. Degradation of structural cell wall components and fermentation profile of ABE production during CPBP (a and c) and CBP (b and d) of AVLR biomass respectively

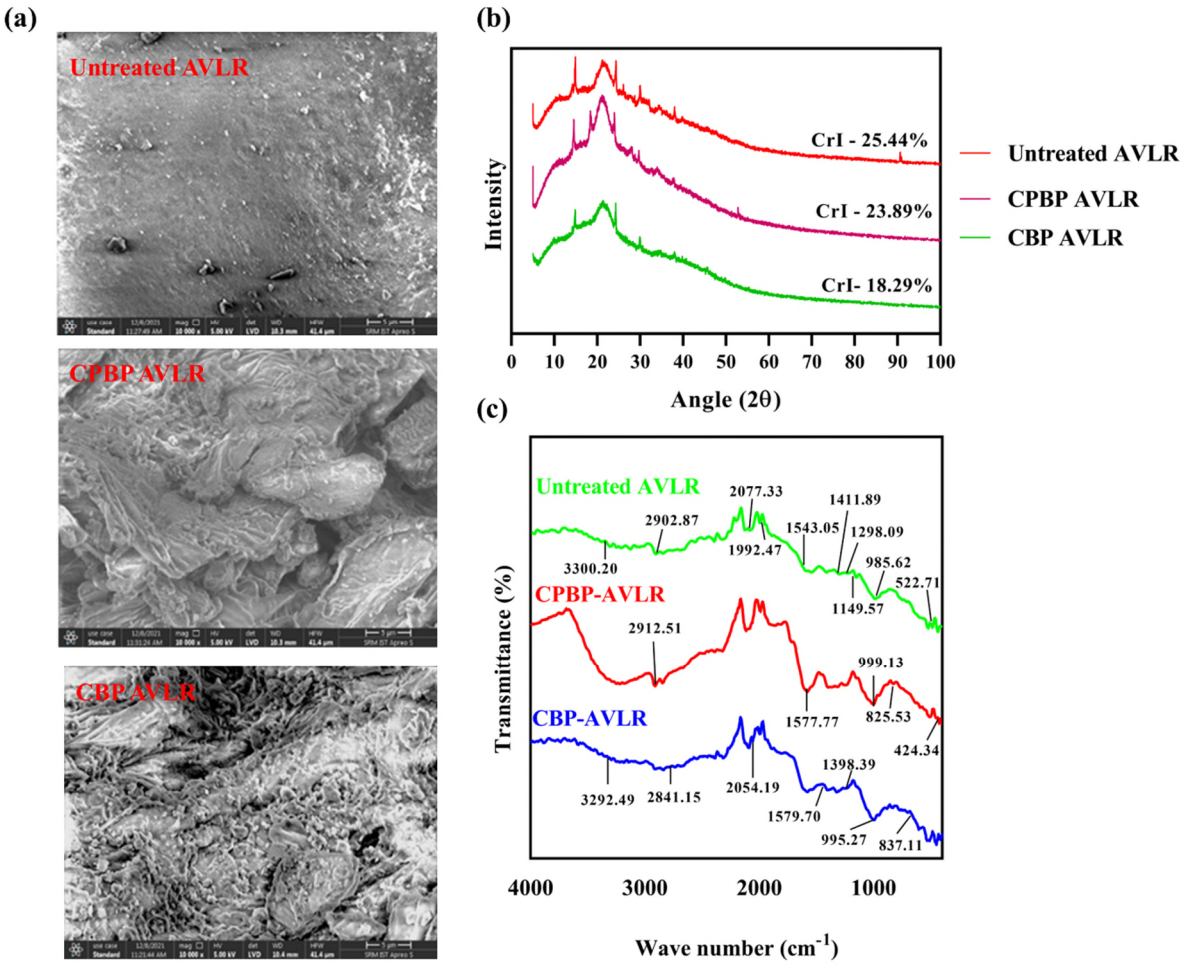


Fig. 8. SEM (a), XRD (b) and FTIR (c) analysis of untreated and treated AVLR biomass under different process strategies

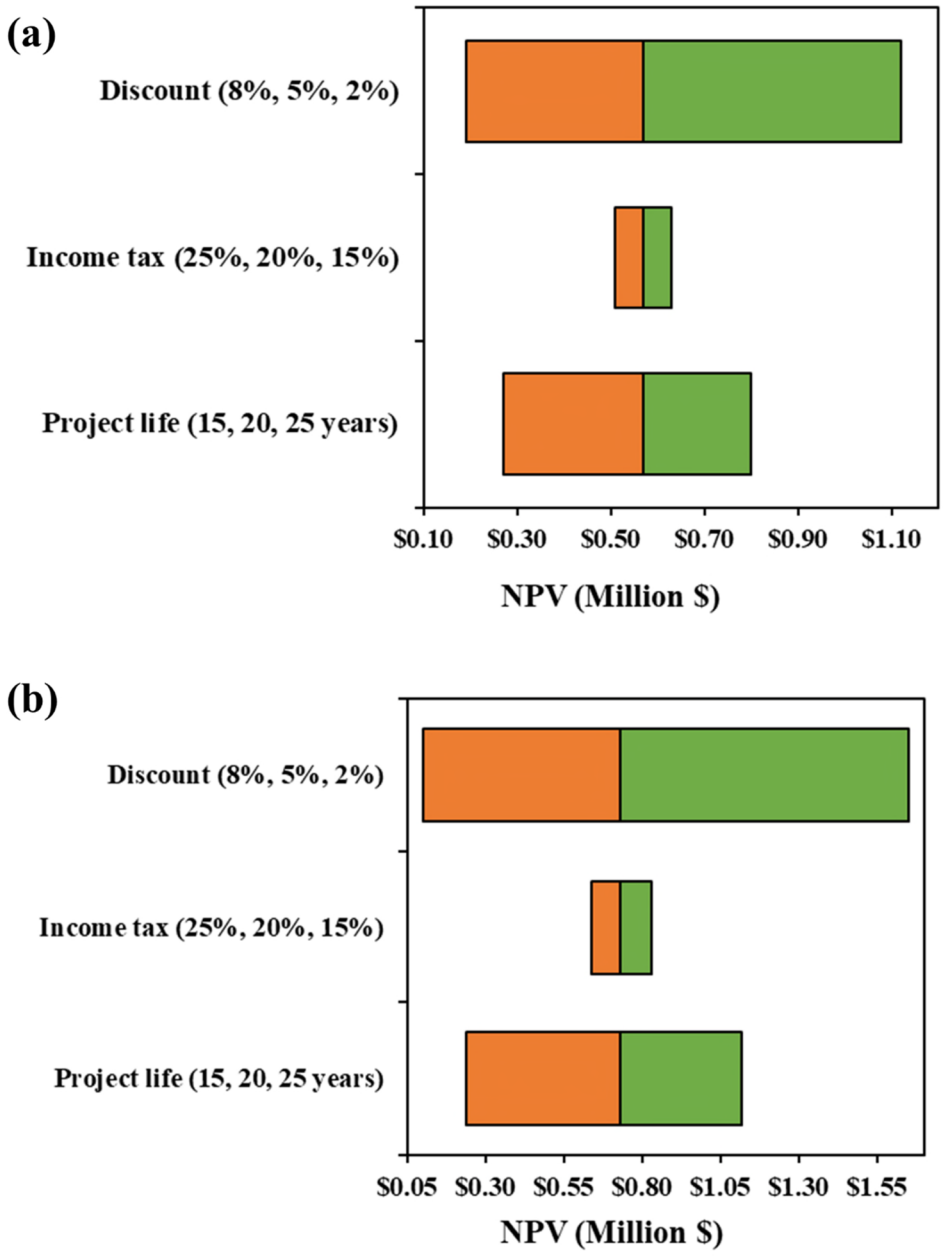
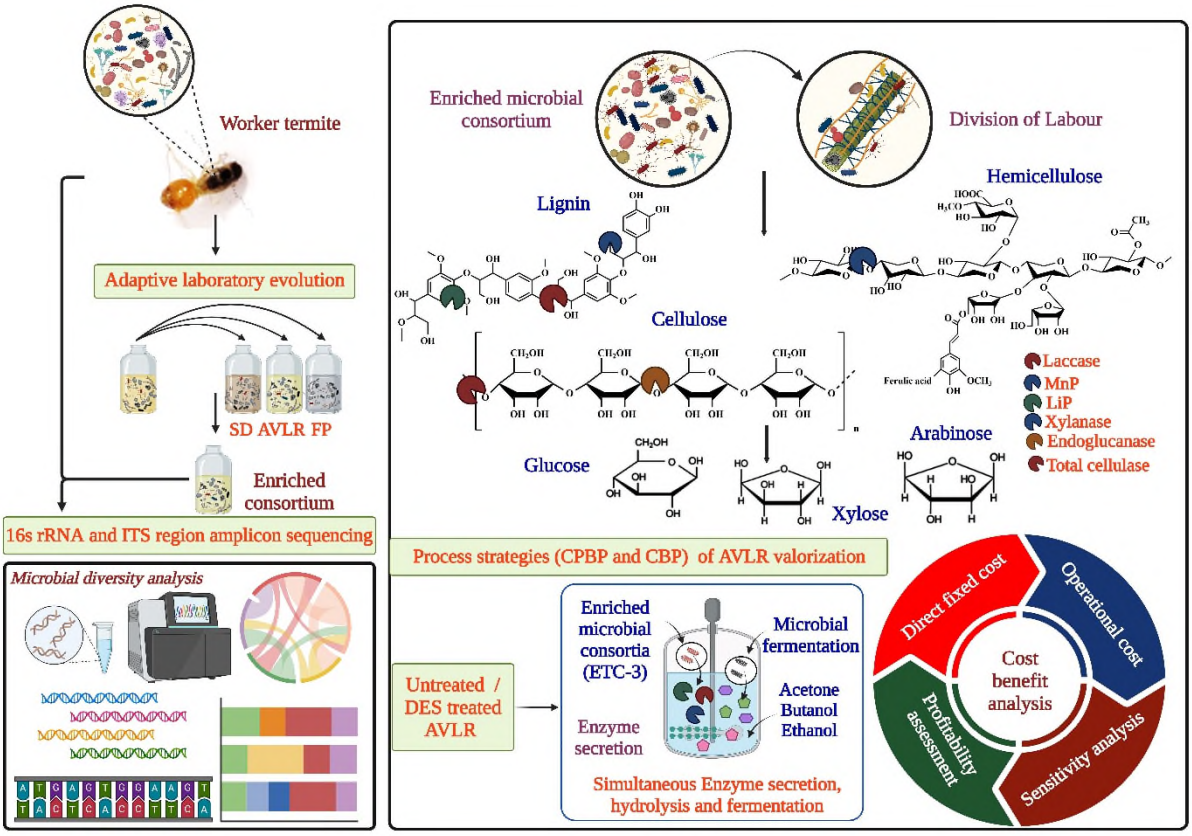


Fig. 9. Sensitivity analysis of NPV for different process strategies (a) CPBP and (b) CBP



Graphical abstract



https://dspace.org/

Advanced lignocellulose bioprocessing for Aloe vera leaf rind through novel termite gut microbiome consortia for acetone butanol ethanol (ABE) production: metagenomics insights and process economic analysis

Rajeswari, Gunasekaran; Kumar, Vinod; Jacob, Samuel

2025-08-01
Elsevier
https://doi.org/10.1016/j.ijbiomac.2025.145691
Rajeswari G, Kumar V, Jacob S. (2025) Advanced lignocellulose bioprocessing for Aloe vera leaf rind through novel termite gut microbiome consortia for acetone butanol ethanol (ABE) production: metagenomics insights and process economic analysis. International Journal of Biological Macromolecules, Volume 319, Part 4, August 2025, Article number 145691

Downloaded from a DSpace repository. https://dspace.org/